

Policy Optimization in the Linear Quadratic Gaussian Problem: A Frequency Domain Perspective

Haoran Li* Xun Li† Yuan-Hua Ni‡ Xuebo Zhang§

January 12, 2026

Abstract

The Linear Quadratic Gaussian (LQG) problem is a classic and widely studied model in optimal control, providing a fundamental framework for designing controllers for linear systems subject to process and observation noises. In recent years, researchers have increasingly focused on directly parameterizing dynamic controllers and optimizing the LQG cost over the resulting parameterized set. However, this parameterization typically gives rise to a highly non-convex optimization landscape for the resulting parameterized LQG problem. To our knowledge, there is currently no general method for certifying the global optimality of candidate controller parameters in this setting. Moreover, most existing numerical methods lack rigorous guarantees of global convergence. In this work, we address these gaps with the following contributions. First, we derive a necessary and sufficient condition for the global optimality of stationary points in a parameterized LQG problems. This condition reduces the verification of optimality to a test of the controllability and observability for a novel, specially constructed transfer function, yielding a precise and computationally tractable certificate. Furthermore, our condition provides a rigorous explanation for why traditional parameterizations can lead to suboptimal stationary points. Second, we elevate the controller parameter space from conventional finite-dimensional settings to the infinite-dimensional \mathcal{RH}_∞ space and develop a gradient-based algorithm in this setting, for which we provide a theoretical analysis establishing global convergence. Finally, representative numerical experiments validate the theoretical findings and demonstrate the practical viability of the proposed approach. Additionally, the appendix section explores a data-driven extension to the model-free setting, where we outline a parameter estimation scheme and demonstrate its practical viability through numerical simulation.

Keywords: Linear Quadratic Gaussian control, policy optimization, stationary points, linear fractional transformation

1 Introduction

In recent years, both theoretical advances and the widespread adoption of policy optimization methods in reinforcement learning (RL) [18, 29, 26] have motivated a growing interest in applying policy optimization approaches to classic optimal control problems. Among these control problems, linear quadratic (LQ) formulations—including the Linear Quadratic Regulator (LQR) and Linear Quadratic Gaussian (LQG)—have become principal subjects of theoretical investigation for policy optimization methods, due to their foundational importance in both theory and practice [4, 3, 42].

For LQR problem, the explicit form and the global uniqueness of the optimal policy, as well as the problem’s hidden convexity facilitate rigorous theoretical analysis of policy optimization methods [9, 27]. As a result, LQR problem serves as an important paradigm for studying the convergence and

*Department of Applied Mathematics, The Hong Kong Polytechnic University, China. Email: 25039255r@connect.polyu.hk

†Department of Applied Mathematics, The Hong Kong Polytechnic University, China. Email: li.xun@polyu.edu.hk. This author is supported by RGC of Hong Kong grants 15226922 and 15225124, and partially from PolyU 4-ZZVB and 4-ZZP4.

‡College of Artificial Intelligence, Nankai University, Tianjin, China. Email: yhni@nankai.edu.cn

§College of Artificial Intelligence, Nankai University, Tianjin, China. Email: zhangxuebo@nankai.edu.cn

sample complexity of policy optimization methods. Furthermore, the analytical techniques and insights developed from policy optimization in LQR problem offer powerful tools and conceptual frameworks for more challenging problems, such as LQG problem and other areas in optimal and robust control [15, 30, 14]. However, when moving from LQR problem to the more general LQG problem, which features partial state observation as well as process and measurement noises, most of the benign properties in LQR problem no longer hold. The optimization landscape of LQG problem is highly nonconvex and more difficult to characterize, making rigorous theoretical analysis of policy optimization methods much more challenging [39, 30]. In light of these differences, we briefly review key theoretical progress on policy optimization for both LQR and LQG problems, with emphasis on the distinctive analytical features and technical challenges of each case.

In recent years, applying policy optimization methods to LQR problem has drawn significant research interest, with a strong focus on rigorously establishing global convergence guarantees. Fatkhullin and Polyak (2020) [7] pioneer the analysis of gradient-based algorithm convergence rates for continuous-time and output feedback LQR, establishing linear convergence in these contexts. Fazel et al. (2018) [9] propose a model-free policy gradient approach for discrete-time LQR. Their work provides convergence guarantees for various policy gradient methods with different update rules (natural gradient descent, gradient descent, and Gauss-Newton step), as well as the sample complexity of gradient estimation via zeroth-order methods. Mohammadi et al. (2019) [19] extend the theoretical guarantees established by Fazel et al. (2018) to the continuous-time case. The above studies systematically deepen our understanding of the optimization landscape for LQR problems. Furthermore, the analytical techniques and convergence tools developed in the policy optimization methods in LQR problem provide a crucial theoretical foundation and motivating methodology for using policy optimization methods to tackling more general LQ problems. Beyond standard LQR, a variety of works generalize analysis to LQR variants with additional constraints or more complex system structures, such as $\mathcal{H}_2/\mathcal{H}_\infty$ mixed objectives [15], Markov jump systems [16], risk constraints [37], and finite horizon problems [13]. Collectively, these studies further enrich the theoretical understanding of policy optimization in LQ problems and show that many analytical tools from standard LQR problem can be adapted to the broader contexts.

Researchers begin exploring the applicability boundaries of policy optimization methods in LQG problem, building upon their successful application in solving LQR problem. However, the convergence guarantees for policy optimization methods in solving LQR problems cannot be easily extended the LQG setting. Compared with LQR, LQG problem is subject to partial state observation as well as process and measurement noises, and its optimal solution is a dynamic regulator. These differences make the analysis of LQG problem more challenging than that of LQR. In response to these increasing complexities, prior work has primarily focused on two directions: the analysis of optimization landscape [30, 6, 41] and convex reformulation techniques [32, 39, 40].

Tang et al. (2021) [30] provide an analysis of LQG connectivity, demonstrating through convex parameterization and manifold theory that the solution space consists of two connected components, each containing global optima. The work also identifies differences between LQG and LQR problems: the stationary points of LQG problem include many saddle points, suggesting that gradient-based methods may converge to suboptimal stationary point, and the lack of coerciveness and inconsistent stability margins in the LQG cost functional can potentially lead to policy gradient method divergence. They further show that stationary points become optimal when the Lyapunov equations admit non-degenerate solutions. Subsequent research further explores the optimality conditions of LQG problem's stationary points. Duan et al. (2024) [6] extend the analysis of [30] to the Dynamical LQR (DLQR) problem, and their numerical experiments demonstrate that standard policy optimization methods may fail to converge to optimal policies under certain parameter settings. In the follow-up work [41], stochastic perturbations are introduced into the LQG setting to help policy optimization methods escape strict saddle points (i.e., stationary points with indefinite Hessians). Although this approach increases the probability of convergence, guarantees on the convergence rate of policy optimization methods are not provided.

Notably, the optimal dynamic filtering problem, as a simplified variant of LQG problem, gives rise to policy optimization methods with global convergence and sublinear convergence rates. Building on this problem, Umenberger et al. (2022) [32] propose the Differential Convex Lifting (DCL) method, which extends earlier convex parameterization theory. Their approach embeds the original optimization variables into an extended space and constructs a diffeomorphic mapping between the extended problem and a convex formulation, guaranteeing that all the stationary points in the extended domain correspond

to globally optimal solutions of optimal dynamic filtering problem. Building on this theory, they prove that the optimal dynamic filtering process satisfies the weak Polyak-Lojasiewicz (PL) condition and further propose a transformation technique to ensure the coerciveness of the cost functional. The main theoretical tools for this work are drawn from the broader field of robust optimal control. In this line of research, Scherer et al. [28] develop convex parameterization methods for LQG problem, which form the basis of DCL. However, the effectiveness of these approaches is often restricted by their heavy reliance on accurate system models, which limits their applicability in structured \mathcal{H}_∞ synthesis [2] and risk-sensitive scenarios [36]. These limitations, in turn, have motivated a recent surge of research on data-driven policy optimization methods. As a result, to address nonconvex problems such as LQG and dynamic filtering, researchers have begun to integrate policy optimization methods with convex parameterization theory to leverage the strengths of both methodologies. Zheng et al. (2023,2024) [39, 40] subsequently generalize DCL to LQG and \mathcal{H}_∞ controller optimization. Their work demonstrates that the LQG problem is equivalent to a linearly constrained convex optimization problem. However, the construction of this problem requires accurate system models and assumptions of invertibility for model parameters.

The preceding theory on LQG problem has largely been confined to time-domain analysis. To overcome the known limitations of classic approaches, we re-examine the problem from a modern, system-level perspective using frequency-domain tools and linear fractional transformations (LFTs). This viewpoint allows us to move beyond treating the controller as a simple set of parameters and instead analyze its systemic interactions with the plant, and uncovers fundamental distinctions between LQR and LQG that explain long-standing challenges in the field. Our main contributions are as follows.

- **Theoretical Insight: A Necessary and Sufficient Condition for Global Optimality**

The Gap. It is widely observed that policy gradient methods for LQG problem often become trapped in suboptimal stationary points [30, 41]. This contrasts sharply with LQR problem, where direct parameterization of controller gain is known to yield an optimization landscape with a unique, globally optimal stationary point. This discrepancy raises an open question: why is direct controller parameterization so successful for LQR, but induces numerous suboptimal stationary points for the seemingly similar LQG problem? Meanwhile, the tools to certify that a point is globally optimal in LQG problem under direct parameterization are incomplete, as a complete characterization of its global optima (i.e., a necessary and sufficient condition) is still lacking [41, 39, 28].

Our Contribution. We resolve the two issues by establishing the necessary and sufficient condition for global optimality under direct parameterization. This provides a tractable criterion to certify whether any given controller is globally optimal for LQG problem. Leveraging this complete characterization, we reveal the root cause of suboptimal stationary points in LQG problem is that the direct parameterization acts as a projection, while preserving the unique minimum of the optimization landscape for LQR problem, destroys the benign structure of the objective functional of LQG problem. This provides a rigorous explanation for the pitfalls of applying direct parameterization to LQG control.

- **Algorithmic Contribution: A Globally Convergent Gradient-Based Algorithm in \mathcal{RH}_∞ Space**

The Limitation of Existing Methods. Current approaches that provide theoretical guarantees for LQG problem typically operate by transforming the controller search space. These established methods can be classified into two main categories:

1. The first category of methods involves approximating the Youla parameterization with a fixed, finite-order model. This reduces the problem to a tractable, finite-dimensional convex program [38]. However, selecting a controller order a priori introduces an inherent approximation error. Consequently, while the algorithm finds an optimal solution within the chosen subspace, this solution is for an approximated problem, creating a trade-off between controller complexity and suboptimality.
2. The second category of methods reformulate LQG problem into a convex program (e.g., an semi-definite program), which can yield the exact global solution [39]. The applicability of these methods, however, relies on several stringent prerequisites, such as the requirement of a full and precise model of system dynamics and prior knowledge of noise statistics.

Our Contribution. In this work, we develop a gradient-based algorithm that operates directly in the \mathcal{RH}_∞ space, bypassing the need for initial truncation. Our algorithm performs iterative updates in the function space. By not confining the search to a fixed-order subspace, this approach avoids the intrinsic approximation error associated with truncation methods.

We provide the global convergence guarantee for the algorithm and characterize its convergence rate. The framework can also be extended to a model-free setting where it can learn from input/output data.

This paper is organized as follows Section 2 introduces LQG problem. Section 3 analyzes the optimality condition for stationary points. Section 4 presents a comparative analysis between LQR and LQG problems, highlighting structural differences under output feedback constraints. Section 5 develops a gradient-based optimization method with convergence analysis. Section 6 validates the theoretical findings and demonstrate the practical viability of the proposed approach via some numerical experiments. Finally, Appendix A explores a potential extension of our algorithm to the model-free setting, outlining a parameter estimation approach whose effectiveness is also validated in Section 6.

Notation. Let $\mathbb{N} = \{0, 1, 2, 3, \dots\}$ denote the set of natural numbers, and \mathbb{R} and \mathbb{C} be the sets of real and complex numbers, respectively. For any positive integers m and n , we denote by \mathbb{R}^m the set of real m -dimensional column vectors, and by $\mathbb{R}^{m \times n}$ and $\mathbb{C}^{m \times n}$ the set of real and complex $m \times n$ matrices, respectively. We let I_m denote the $m \times m$ identity matrix, $e_{m \times n}(i, j)$ the $m \times n$ matrix with 1 the (i, j) entry and 0 elsewhere for $1 \leq i \leq m$, $1 \leq j \leq n$, and $0_{m \times n}$ the $m \times n$ zero matrix. Given integers $1 \leq i \leq m$ and $1 \leq j \leq n$, define

$$\mathbb{R}^{m \times n | i \times j} = \left\{ A \in \mathbb{R}^{m \times n} : A = \begin{bmatrix} 0_{i \times j} & * \\ * & * \end{bmatrix} \right\}$$

as the set of $m \times n$ real matrices whose top-left $i \times j$ block is zero. Define the operator

$$\mathbf{e}_{m \times n}(\cdot, i, j) : \mathbb{R}^{m \times n} \rightarrow \mathbb{R}^{m \times n | i \times j}$$

which, for any $A \in \mathbb{R}^{m \times n}$, sets the entries in the top-left $i \times j$ block of A to zero, and leaves all other entries unchanged. For any matrix $A \in \mathbb{C}^{m \times n}$, A^\top , A^* , $\|A\|$, $\|A\|_F$ denote its transpose, its conjugate transpose, its spectral (operator) norm, and its Frobenius norm, respectively. The smallest and largest singular values of A are denoted as $\sigma_{\min}(A)$ and $\sigma_{\max}(A)$, respectively. If A is square and invertible, A^{-1} denotes its inverse.

Consider a continuous-time, linear time-invariant (LTI) system:

$$\begin{aligned} \dot{x}(t) &= Ax(t) + Bu(t), \\ y(t) &= Cx(t) + Du(t), \end{aligned} \tag{1}$$

where A , B , C , and D are real matrices with compatible dimensions. The corresponding transfer function matrix is

$$G(s) = C(sI - A)^{-1}B + D,$$

where $s \in \mathbb{C}$ is the Laplace variable. For notational convenience, we also represent this transfer function using the compact state-space form:

$$\left[\begin{array}{c|c} A & B \\ \hline C & D \end{array} \right]. \tag{2}$$

For a stable (i.e., all its poles have negative real parts), proper (i.e., $\lim_{s \rightarrow \infty} G(s)$ is a finite constant matrix; strictly proper, i.e., $\lim_{s \rightarrow \infty} G(s) = 0$) transfer function matrix $G(s)$, the \mathcal{H}_2 and \mathcal{H}_∞ norms, denoted as $\|G\|_{\mathcal{H}_2} := \int_{-\infty}^{\infty} \text{tr}(G^*(j\omega)G(j\omega)) \frac{d\omega}{2\pi}$ and $\|G\|_{\mathcal{H}_\infty} := \sup_{0 \leq \omega < \infty} \sigma_{\max}(G(j\omega))$, are defined in [42]. Let \mathcal{RH}_∞ (resp., $\mathcal{RH}_{\infty,0}$) denote the set of all the proper (resp., strictly proper), stable, rational (i.e., each of its entries is a ratio of polynomials in $s \in \mathbb{C}$) transfer function matrices. For $G, H \in \mathcal{RH}_\infty$ with the same input and output dimensions, their \mathcal{H}_2 inner product is defined as

$$\langle G, H \rangle_{\mathcal{H}_2} = \int_{-\infty}^{\infty} \text{tr}(G^*(j\omega)H(j\omega)) \frac{d\omega}{2\pi}.$$

This definition follows [42]. The mixed second-order directional derivative $D_{\mathbf{u}}D_{\mathbf{v}}f(\mathbf{x})$ is defined as

$$D_{\mathbf{u}}D_{\mathbf{v}}f(\mathbf{x}) := \sum_{i,j=1}^n \frac{\partial^2 f}{\partial x_i \partial x_j}(\mathbf{x}) u_i v_j \quad (3)$$

with any second order differentiable function $f : \mathbb{R}^n \rightarrow \mathbb{R}$ and any vectors $\mathbf{u} := (u_1, \dots, u_n), \mathbf{v} = (v_1, \dots, v_n) \in \mathbb{R}^n$,

2 Problem formulation

In this section, we formulate LQG problem as an optimization problem over a class of parameterized control policies. Specifically, the continuous-time LQG problem [31] is

$$\begin{aligned} \min_{u_t} \lim_{T \rightarrow \infty} \frac{1}{T} \mathbb{E} \left[\int_0^T (x_t^\top Q x_t + u_t^\top R u_t) dt \right], \\ \text{s.t.} \quad \begin{cases} \dot{x}_t = A x_t + B u_t + \omega_t, \\ y_t = C x_t + v_t, \end{cases} \end{aligned} \quad (4)$$

where $A \in \mathbb{R}^{n \times n}$, $B \in \mathbb{R}^{n \times m_1}$, and $C \in \mathbb{R}^{m_2 \times n}$ are system matrices. The input u_t is allowed to depend on all the past observation y_τ , $\tau \leq t$. The noise processes $\{\omega_t\}$ and $\{v_t\}$ are mutually independent Gaussian white noise processes with intensity matrices $\mathcal{W} \succ 0$ and $\mathcal{V} \succ 0$, respectively. The weighting matrices $Q \succ 0$ and $R \succ 0$ define the quadratic performance index. A well-known optimal controller of (4) is constructed based on the solutions to the following Riccati equations

$$\begin{aligned} A^\top P + P A - P B R^{-1} B^\top P + Q = 0, \quad K = R^{-1} B^\top P, \\ A H + H A^\top - H C^\top \mathcal{V}^{-1} C H + \mathcal{W} = 0, \quad L = H C^\top \mathcal{V}^{-1}. \end{aligned} \quad (5)$$

It should be noted that under the stabilizability and detectability assumptions each of (5) admits a unique positive definite solution. The optimal feedback gain K and the estimator gain L are subsequently used to construct the optimal controller:

$$\begin{aligned} \dot{\hat{x}}_t &= (A - B K - L C) \hat{x}_t + L y_t, \\ u_t &= -K \hat{x}_t. \end{aligned} \quad (6)$$

The optimality of controller in (6) follows from the known separation principle [42].

While LQG problem admits the explicit optimal solution, real-world scenarios frequently involve model uncertainty or additional constraints that preclude closed-form solutions. To address these challenges, it has become common practice to parameterize controllers and synthesize them via policy optimization, enabling data-driven and gradient-based approaches. Motivated by these considerations, recent literature on LQG controller synthesis and policy optimization [39, 41] investigates the set of all the controllers admitting the following parameterized state-space realization:

$$\begin{cases} \dot{\hat{x}}_t = A_{\mathcal{K}} \hat{x}_t + B_{\mathcal{K}} y_t, \\ u_t = C_{\mathcal{K}} \hat{x}_t, \end{cases} \quad \text{with } A_{\mathcal{K}} \in \mathbb{R}^{q \times q}, B_{\mathcal{K}} \in \mathbb{R}^{q \times m_2}, C_{\mathcal{K}} \in \mathbb{R}^{m_1 \times q}, \quad (7)$$

where q is chosen so that this class of parameterizations encompasses the optimal LQG controller (6).

Building on this parameterization, the previous works [39, 41] have proposed the following policy optimization problem over parameterized dynamic controllers (7) for the LQG setting

$$\begin{aligned} \min_{\mathcal{K} \in \mathbb{K}_q} J(\mathcal{K}) &:= \lim_{T \rightarrow \infty} \frac{1}{T} \mathbb{E} \left[\int_0^T (x_t^\top Q x_t + u_t^\top R u_t) dt \right] \\ \text{s.t.} \quad &\begin{cases} \dot{x}_t = A x_t + B u_t + \omega_t, \\ \dot{\hat{x}}_t = A_{\mathcal{K}} \hat{x}_t + B_{\mathcal{K}} y_t, \\ y_t = C x_t + v_t, \\ u_t = C_{\mathcal{K}} \hat{x}_t, \end{cases} \end{aligned} \quad (8)$$

where

$$\mathcal{K} = \begin{bmatrix} 0 & C_{\mathcal{K}} \\ B_{\mathcal{K}} & A_{\mathcal{K}} \end{bmatrix} \in \mathbb{R}^{(q+m_1) \times (q+m_2)} \quad (9)$$

parameterizes the dynamic controller, and \mathbb{K}_q denotes the set of all such \mathcal{K} that stabilize the corresponding closed-loop system (8), thus ensuring the problem is well-posed. This parameterization is chosen so that the class \mathbb{K}_q contains, in particular, the optimal LQG controller.

3 The optimal condition of problem (8)

In this section, we first introduce some basic properties of problem (8), and then establish necessary and sufficient condition for a feasible point of problem (8) to be globally optimal.

3.1 The properties of problem (8)

To facilitate analysis and computation, it is convenient to represent the closed-loop system (8) using an augmented state variable $\xi_t = [x_t^\top \hat{x}_t^\top]^\top$. With this augmented state variable, the closed-loop system dynamics can be expressed as

$$\dot{\xi}_t = \underbrace{\begin{bmatrix} A & BC_{\mathcal{K}} \\ B_{\mathcal{K}}C & A_{\mathcal{K}} \end{bmatrix}}_{\mathcal{A}} \xi_t + \begin{bmatrix} I & 0 \\ 0 & B_{\mathcal{K}} \end{bmatrix} \begin{bmatrix} \omega_t \\ v_t \end{bmatrix}. \quad (10)$$

Thus for any $\mathcal{K} \in \mathbb{K}_q$, the performance index in (8) admits two equivalent representations in terms of solutions to two Lyapunov equations:

$$\begin{aligned} J(\mathcal{K}) &= \text{tr} \left(\begin{bmatrix} \mathcal{W} & 0 \\ 0 & B_{\mathcal{K}} \mathcal{V} B_{\mathcal{K}}^\top \end{bmatrix} \mathcal{P}_{\mathcal{K}} \right) \\ &= \text{tr} \left(\begin{bmatrix} Q & 0 \\ 0 & C_{\mathcal{K}}^\top R C_{\mathcal{K}} \end{bmatrix} \Sigma_{\mathcal{K}} \right), \end{aligned} \quad (11)$$

where

$$\mathcal{P}_{\mathcal{K}} = \begin{bmatrix} P_{11}^{\mathcal{K}} & P_{12}^{\mathcal{K}} \\ P_{21}^{\mathcal{K}} & P_{22}^{\mathcal{K}} \end{bmatrix}, \quad \Sigma_{\mathcal{K}} = \begin{bmatrix} \Sigma_{11}^{\mathcal{K}} & \Sigma_{12}^{\mathcal{K}} \\ \Sigma_{21}^{\mathcal{K}} & \Sigma_{22}^{\mathcal{K}} \end{bmatrix}$$

solve the Lyapunov equations

$$\begin{aligned} \mathcal{A}^\top \mathcal{P}_{\mathcal{K}} + \mathcal{P}_{\mathcal{K}} \mathcal{A} &= - \begin{bmatrix} Q & 0 \\ 0 & C_{\mathcal{K}}^\top R C_{\mathcal{K}} \end{bmatrix}, \\ \mathcal{A} \Sigma_{\mathcal{K}} + \Sigma_{\mathcal{K}} \mathcal{A}^\top &= - \begin{bmatrix} \mathcal{W} & 0 \\ 0 & B_{\mathcal{K}} \mathcal{V} B_{\mathcal{K}}^\top \end{bmatrix}, \end{aligned} \quad (12)$$

and, for clarity, the block matrices have the following dimensions:

$$P_{11}^{\mathcal{K}}, \Sigma_{11}^{\mathcal{K}} \in \mathbb{R}^{n \times n}, \quad P_{12}^{\mathcal{K}}, \Sigma_{12}^{\mathcal{K}} \in \mathbb{R}^{n \times q}, \quad P_{22}^{\mathcal{K}}, \Sigma_{22}^{\mathcal{K}} \in \mathbb{R}^{q \times q}.$$

Thus, the search for optimal controllers reduces to identifying the minimizer of $J(\mathcal{K})$ over \mathbb{K}_q . For simplicity, we let $\mathcal{K}^* \in \mathbb{K}_q$ as a stationary point, if the gradient of $J(\mathcal{K}^*)$ at \mathcal{K}^* satisfies

$$\nabla J(\mathcal{K}^*) = 0.$$

While policy gradient and related direct optimization methods have been widely applied to problem (8) [30, 41], they often struggle with convergence and become trapped in suboptimal stationary points. This issue stems in part from a critical theoretical gap: no definitive conditions exist to verify the global optimality of a stationary point. Most existing results offer only one-sided conditions—that is, necessary or sufficient, but not both—leaving the status of such points largely uncharacterized.

Our work systematically addresses these challenges through three interconnected contributions. First, in Section 3, we establish a necessary and sufficient condition for a point to be a global optimum

of problem (8). This rigorous criterion provides the first definitive tool to verify global optimality. Second, leveraging this characterization, our analysis in Section 4 reveals the root cause of suboptimal stationary points in the optimization landscape of problem (8). Finally, armed with this deep theoretical understanding, we introduce in Section 5 a novel gradient-based algorithm to solve problem (8). By operating within a parameterization that ensures a broad class of admissible controllers, our algorithm is specifically designed to circumvent the identified landscape challenges and is proven to converge to the optimal value.

3.2 Optimal condition analysis

The challenge of certifying optimality for stationary points in problem (8) has spurred significant recent research. A notable line of work involves leveraging convex parameterization techniques to reveal hidden convex structures within the problem [39, 40]. These developments have deepened on the understanding of optimization landscape and, crucially, enabled the certification of global optimality for certain stationary points under specific conditions.

Lemma 3.1. [40] *If $q = n$ and \mathcal{K}^* is a stationary point of problem (8) that satisfies*

$$\mathcal{P}_{\mathcal{K}^*} = \begin{bmatrix} P_{11}^{\mathcal{K}^*} & P_{12}^{\mathcal{K}^*} \\ P_{21}^{\mathcal{K}^*} & P_{22}^{\mathcal{K}^*} \end{bmatrix} \succ 0, \quad \det |P_{12}^{\mathcal{K}^*}| \neq 0, \quad (13)$$

or

$$\Sigma_{\mathcal{K}^*} = \begin{bmatrix} \Sigma_{11}^{\mathcal{K}^*} & \Sigma_{12}^{\mathcal{K}^*} \\ \Sigma_{21}^{\mathcal{K}^*} & \Sigma_{22}^{\mathcal{K}^*} \end{bmatrix} \succ 0, \quad \det |\Sigma_{12}^{\mathcal{K}^*}| \neq 0, \quad (14)$$

then \mathcal{K}^* is an optimal solution to problem (8).

However, the sufficient conditions provided by Lemma 3.1 and related results [39, 40] are applicable only to a specific subset of controllers in \mathbb{K}_q that satisfy the structural constraints (13) or (14). Consequently, for any stationary point corresponding to a controller that fails to meet these strict requirements, existing convex reformulation techniques cannot determine whether it is globally optimal.

To overcome this fundamental limitation and establish a truly general criterion, our work pivots to a different approach founded on frequency-domain analysis and linear fractional transformations (LFTs). As a foundational step for this analysis, we first reformulate problem (8) as an equivalent \mathcal{H}_2 optimization problem. This reformulation provides the necessary framework to derive our necessary and sufficient condition without relying on the restrictive structural assumptions of prior works. Let

$$\begin{aligned} \min_{\mathcal{K} \in \mathbb{K}_q} \quad & \|G_{\mathcal{K}}\|_{\mathcal{H}_2}^2 \\ \text{s.t.} \quad & G_{\mathcal{K}}(s) = \mathcal{C}(sI - \mathcal{A})^{-1}\mathcal{B} \end{aligned} \quad (15)$$

with

$$\mathcal{A} = \begin{bmatrix} A & BC_{\mathcal{K}} \\ B_{\mathcal{K}}C & A_{\mathcal{K}} \end{bmatrix}, \mathcal{C} = \begin{bmatrix} Q^{\frac{1}{2}} & 0 \\ 0 & R^{\frac{1}{2}}C_{\mathcal{K}} \end{bmatrix}, \mathcal{B} = \begin{bmatrix} \mathcal{W}^{\frac{1}{2}} & 0 \\ 0 & B_{\mathcal{K}}\mathcal{V}^{\frac{1}{2}} \end{bmatrix}. \quad (16)$$

Lemma 3.2. *The policy optimization problem (8) is equivalent to the \mathcal{H}_2 norm optimization problem (15) in the sense that both problems have the same feasible set, and the two cost functionals are equal for any $\mathcal{K} \in \mathbb{K}_q$.*

Proof. Note that the feasible set of (15) is the same as that of problem (8). Then, for any $\mathcal{K} \in \mathbb{K}_q$ and Parseval's theorem, the objective $\|G_{\mathcal{K}}\|_{\mathcal{H}_2}^2$ admits an equivalent time-domain representation

$$\|G_{\mathcal{K}}\|_{\mathcal{H}_2}^2 = \text{tr} \left(\int_0^\infty \mathcal{B}^\top e^{\mathcal{A}^\top t} \mathcal{C}^\top \mathcal{C} e^{\mathcal{A}t} \mathcal{B} dt \right). \quad (17)$$

As established in (11) above, this expression equals to

$$\text{tr} \left(\begin{bmatrix} \mathcal{W} & 0 \\ 0 & B_{\mathcal{K}}\mathcal{V}B_{\mathcal{K}}^\top \end{bmatrix} \mathcal{P}_{\mathcal{K}} \right) = J(\mathcal{K}). \quad (18)$$

This completes the proof. \square

Building on the equivalence between problem (8) and problem (15), we analyze the optimality condition of problem (8) by considering the perturbations for the \mathcal{H}_2 norm optimization problem. Let \mathcal{K} be any controller parameter belonging \mathbb{K}_q , and consider a perturbed controller $\mathcal{K}' = \mathcal{K} + \Delta\mathcal{K} \in \mathbb{K}_q$, where the perturbation $\Delta\mathcal{K}$ is defined as

$$\begin{aligned} \Delta C_{\mathcal{K}} &:= C_{\mathcal{K}'} - C_{\mathcal{K}}, \quad \Delta B_{\mathcal{K}} := B_{\mathcal{K}'} - B_{\mathcal{K}}, \quad \Delta A_{\mathcal{K}} := A_{\mathcal{K}'} - A_{\mathcal{K}}, \\ \Delta\mathcal{K} &:= \begin{bmatrix} 0 & \Delta C_{\mathcal{K}} \\ \Delta B_{\mathcal{K}} & \Delta A_{\mathcal{K}} \end{bmatrix}. \end{aligned}$$

Unlike conventional optimization methods, we explicitly extract the controller perturbation $\Delta\mathcal{K}$ as an external feedback block. Specifically, for a perturbed controller $\mathcal{K}' = \mathcal{K} + \Delta\mathcal{K}$, the input-output behavior [42] of the closed-loop system with $G_{\mathcal{K}'}$ can be reformulated as a feedback interconnection between the nominal system $G_{\mathcal{K}}$ (parameterized by \mathcal{K}) and the perturbation block $\Delta\mathcal{K}$, with the interconnection mediated by the auxiliary signals $(\hat{y}_{1t}, \hat{u}_{1t}, y_t, y_{3t})$ [19]. Here, (y_t, y_{3t}) serves as the output signals from $G_{\mathcal{K}}$ to $\Delta\mathcal{K}$, while $(\hat{y}_{1t}, \hat{u}_{1t})$ is the corresponding feedback input. This reformulation allows us to analyze the system's performance using the deterministic \mathcal{H}_2 norm, which corresponds to the expected steady-state variance in the original LQG problem. With a slight abuse of notation, the symbols ω_t and v_t are now reinterpreted as deterministic exogenous inputs rather than stochastic noise processes. This is a standard technique where the statistical properties of the original noise are captured by weighting these new inputs with the Cholesky factors of their respective covariance matrices, $\mathcal{W}^{1/2}$ and $\mathcal{V}^{1/2}$. The resulting LFT representation is given by

$$\begin{bmatrix} \dot{\hat{x}}_t \\ \hat{x}_t \end{bmatrix} = \begin{bmatrix} A & BC_{\mathcal{K}} \\ B_{\mathcal{K}}C & A_{\mathcal{K}} \end{bmatrix} \begin{bmatrix} x_t \\ \hat{x}_t \end{bmatrix} + \begin{bmatrix} \mathcal{W}^{\frac{1}{2}} & 0 & B & 0 \\ 0 & B_{\mathcal{K}}\mathcal{V}^{\frac{1}{2}} & 0 & I \end{bmatrix} \begin{bmatrix} \omega_t \\ v_t \\ \hat{y}_{1t} \\ \hat{u}_{1t} \end{bmatrix}, \quad (19)$$

$$\begin{bmatrix} y_{1t} \\ y_{2t} \\ y_t \\ y_{3t} \end{bmatrix} = \begin{bmatrix} Q^{\frac{1}{2}} & 0 \\ 0 & R^{\frac{1}{2}}C_{\mathcal{K}} \\ C & 0 \\ 0 & I \end{bmatrix} \begin{bmatrix} x_t \\ \hat{x}_t \end{bmatrix} + \begin{bmatrix} 0 & 0 & 0 & 0 \\ 0 & 0 & R^{\frac{1}{2}} & 0 \\ 0 & \mathcal{V}^{\frac{1}{2}} & 0 & 0 \\ 0 & 0 & 0 & 0 \end{bmatrix} \begin{bmatrix} \omega_t \\ v_t \\ \hat{y}_{1t} \\ \hat{u}_{1t} \end{bmatrix}, \quad (20)$$

$$\begin{bmatrix} \hat{y}_{1t} \\ \hat{u}_{1t} \end{bmatrix} = \Delta\mathcal{K} \begin{bmatrix} y_t \\ y_{3t} \end{bmatrix}. \quad (21)$$

This frequency-domain formulation is particularly advantageous for sensitivity and robustness analysis, enabling a systematic investigation of controller optimality condition under perturbations. The corresponding transfer function $G_{\mathcal{K}'}(s)$ is given by the upper LFT

$$G_{\mathcal{K}'}(s) = \mathcal{F}_u(\mathbf{M}_{\mathcal{K}}(s), \Delta\mathcal{K}) = \mathbf{M}_{11}^{\mathcal{K}}(s) + \mathbf{M}_{12}^{\mathcal{K}}(s)\Delta\mathcal{K}(I - \mathbf{M}_{22}^{\mathcal{K}}(s)\Delta\mathcal{K})^{-1}\mathbf{M}_{21}^{\mathcal{K}}(s), \quad (22)$$

where

$$\mathbf{M}_{\mathcal{K}}(s) := \begin{bmatrix} \mathbf{M}_{11}^{\mathcal{K}}(s) & \mathbf{M}_{12}^{\mathcal{K}}(s) \\ \mathbf{M}_{21}^{\mathcal{K}}(s) & \mathbf{M}_{22}^{\mathcal{K}}(s) \end{bmatrix}$$

is the nominal transfer function matrix with realization

$$\begin{aligned} \mathbf{M}_{11}^{\mathcal{K}}(s) &:= \mathcal{C}(sI - \mathcal{A})^{-1}\mathcal{B} = G_{\mathcal{K}}(s), \\ \mathbf{M}_{12}^{\mathcal{K}}(s) &:= \mathcal{C}(sI - \mathcal{A})^{-1} \begin{bmatrix} B & 0 \\ 0 & I \end{bmatrix} + \begin{bmatrix} 0 & 0 \\ R^{\frac{1}{2}} & 0 \end{bmatrix}, \\ \mathbf{M}_{21}^{\mathcal{K}}(s) &:= \begin{bmatrix} C & 0 \\ 0 & I \end{bmatrix} (sI - \mathcal{A})^{-1}\mathcal{B} + \begin{bmatrix} 0 & \mathcal{V}^{\frac{1}{2}} \\ 0 & 0 \end{bmatrix}, \\ \mathbf{M}_{22}^{\mathcal{K}}(s) &:= \begin{bmatrix} C & 0 \\ 0 & I \end{bmatrix} (sI - \mathcal{A})^{-1} \begin{bmatrix} B & 0 \\ 0 & I \end{bmatrix}. \end{aligned} \quad (23)$$

Letting $\Delta G(s) := \mathbf{M}_{12}^{\mathcal{K}}(s)\Delta\mathcal{K}(I - \mathbf{M}_{22}^{\mathcal{K}}(s)\Delta\mathcal{K})^{-1}\mathbf{M}_{21}^{\mathcal{K}}(s)$, the \mathcal{H}_2 norm $\|G_{\mathcal{K}'}\|_{\mathcal{H}_2}$ can be expanded as

$$\|G_{\mathcal{K}'}\|_{\mathcal{H}_2}^2 = \|G_{\mathcal{K}}\|_{\mathcal{H}_2}^2 + 2\langle G_{\mathcal{K}}, \Delta G \rangle_{\mathcal{H}_2} + \mathcal{O}(\|\Delta\mathcal{K}\|^2), \quad (24)$$

where the first-order variation term is

$$\langle G_{\mathcal{K}}, \Delta G \rangle_{\mathcal{H}_2} = \text{tr} \left(\int_{-\infty}^{\infty} G_{\mathcal{K}}^*(j\omega) \mathbf{M}_{12}^{\mathcal{K}}(j\omega) \Delta \mathcal{K} (I - \mathbf{M}_{22}^{\mathcal{K}}(j\omega) \Delta \mathcal{K})^{-1} \mathbf{M}_{21}^{\mathcal{K}}(j\omega) \frac{d\omega}{2\pi} \right). \quad (25)$$

Observing that $G_{\mathcal{K}'}$ is a linear function of $\Delta \mathcal{K} (I - \mathbf{M}_{22}^{\mathcal{K}} \Delta \mathcal{K})^{-1}$, we can express the higher-order term as

$$\mathcal{O}(\|\Delta \mathcal{K}\|^2) = \|\mathbf{M}_{12}^{\mathcal{K}} \Delta \mathcal{K} (I - \mathbf{M}_{22}^{\mathcal{K}} \Delta \mathcal{K})^{-1} \mathbf{M}_{21}^{\mathcal{K}}\|_{\mathcal{H}_2}^2 \geq 0.$$

The nonnegativity of this higher-order term implies that a sufficient condition for \mathcal{K} to be an optimal solution of problem (8) is the vanishing of first-order variation:

$$\langle G_{\mathcal{K}}, \Delta G \rangle_{\mathcal{H}_2} = 0, \quad \forall \mathcal{K}' \in \mathbb{K}_q. \quad (26)$$

This stationarity condition, which we establish in Theorem 3.4 below as the necessary and sufficient condition for global optimality in problem (8), admits a clear frequency-domain interpretation. Our derivation is closely related to the Youla parameterization [33]. However, a key advantage of our LFT-based approach is that it explicitly retains the controller structure from (7). This structural preservation is significant because it builds a direct bridge between classic control theory and modern policy optimization methods [41].

To leverage this frequency-domain perspective and rigorously analyze the stationarity condition (26), we express the \mathcal{H}_2 inner product using residue calculus. The following lemma provides the explicit formula required for our subsequent derivations.

Lemma 3.3. [42] *Let strictly proper real-coefficient rational vector functions $f(s)$ and $g(s)$ be square-integrable with no poles on the purely imaginary axis. Then, the \mathcal{H}_2 inner product $\langle f, g \rangle_{\mathcal{H}_2}$ equals the sum of residues of $f(-s)^\top g(s)$ at poles in the right half-plane: $\text{Res}_{\Re(s) \leq 0} (f(-s)^\top g(s))$.*

Building on Lemma 3.3, we note that the \mathcal{H}_2 inner product between two strictly proper rational functions is zero if one is stable (i.e., all the poles in the open left half-plane), while the other is anti-stable (i.e., all the poles in the open right half-plane); see [42] for more details. This observation enables us to restate the stationarity condition (26) as an equivalent frequency-domain criterion, which we formalize in the following theorem.

Theorem 3.4. *A controller $\mathcal{K} \in \mathbb{K}_q$ is an optimal solution to problem (8) if and only if*

$$(\mathcal{C}_1 - \mathcal{B}_1 \mathcal{P}_{\mathcal{K}})(sI - \mathcal{A})^{-1}(\mathcal{B}_0 - \Sigma_{\mathcal{K}} \mathcal{C}_0) \equiv 0, \quad \forall s \in \mathbb{C} \quad (27)$$

holds, where

$$\mathcal{B}_0 = \begin{bmatrix} 0 & 0 \\ B_{\mathcal{K}} \mathcal{V} & 0 \end{bmatrix}, \quad \mathcal{C}_0 = - \begin{bmatrix} C^\top & 0 \\ 0 & I \end{bmatrix}, \quad \mathcal{B}_1 = - \begin{bmatrix} B^\top & 0 \\ 0 & I \end{bmatrix}, \quad \mathcal{C}_1 = \begin{bmatrix} 0 & RC_{\mathcal{K}} \\ 0 & 0 \end{bmatrix}. \quad (28)$$

Proof. We first prove the sufficiency. According to Lemma 3.3, the \mathcal{H}_2 inner product $\langle G_{\mathcal{K}}, \Delta G \rangle_{\mathcal{H}_2}$ can be computed as the sum of residues of the product of their corresponding transfer functions in the left half-plane:

$$\begin{aligned} & \langle G_{\mathcal{K}}, \Delta G \rangle_{\mathcal{H}_2} \\ &= \text{tr} \left(\int_{-\infty}^{\infty} ((\mathbf{M}_{12}^{\mathcal{K}}(j\omega))^* \mathbf{M}_{11}^{\mathcal{K}}(j\omega) (\mathbf{M}_{21}^{\mathcal{K}}(j\omega))^*) (\Delta \mathcal{K} (I - \mathbf{M}_{22}^{\mathcal{K}}(j\omega) \Delta \mathcal{K})^{-1})^* \frac{d\omega}{2\pi} \right) \\ &= \text{tr} \left(\text{Res}_{\Re(s) \leq 0} \left(((\mathbf{M}_{12}^{\mathcal{K}}(-s))^\top \mathbf{M}_{11}^{\mathcal{K}}(s) (\mathbf{M}_{21}^{\mathcal{K}}(-s))^\top (\Delta \mathcal{K} (I - \mathbf{M}_{22}^{\mathcal{K}}(-s) \Delta \mathcal{K})^{-1})^\top) \right) \right). \end{aligned}$$

Note that $\Delta \mathcal{K} (I - \mathbf{M}_{22}^{\mathcal{K}}(s) \Delta \mathcal{K})^{-1}$ is stable. Thus, if $(\mathbf{M}_{12}^{\mathcal{K}}(-s))^\top \mathbf{M}_{11}^{\mathcal{K}}(s) (\mathbf{M}_{21}^{\mathcal{K}}(-s))^\top$ is anti-stable, their \mathcal{H}_2 inner product must vanish. It remains to show that this property is equivalent to condition (27). To this end, we further examine the explicit structure of $(\mathbf{M}_{12}^{\mathcal{K}}(-s))^\top \mathbf{M}_{11}^{\mathcal{K}}(s) (\mathbf{M}_{21}^{\mathcal{K}}(-s))^\top$. According to the concatenated representation of transfer function, we have

$$\mathbf{M}_{11}^{\mathcal{K}}(s) (\mathbf{M}_{21}^{\mathcal{K}}(-s))^\top = \left[\begin{array}{cc|c} \mathcal{A} & \mathcal{B}\mathcal{B}^\top & \mathcal{B}_0 \\ 0 & -\mathcal{A}^\top & \mathcal{C}_0 \\ \hline -\mathcal{C} & 0 & 0 \end{array} \right].$$

In a same way, we can obtain

$$(\mathbf{M}_{12}^{\mathcal{K}}(-s))^{\top} \mathbf{M}_{11}^{\mathcal{K}}(s) (\mathbf{M}_{21}^{\mathcal{K}}(-s))^{\top} = \left[\begin{array}{ccc|c} -\mathcal{A}^{\top} & \mathcal{C}^{\top} \mathcal{C} & 0 & 0 \\ 0 & \mathcal{A} & \mathcal{B} \mathcal{B}^{\top} & \mathcal{B}_0 \\ 0 & 0 & -\mathcal{A}^{\top} & \mathcal{C}_0 \\ \hline \mathcal{B}_1 & \mathcal{C}_1 & 0 & 0 \end{array} \right]. \quad (29)$$

Using similar transformation to (29)

$$T \left[\begin{array}{ccc|c} -\mathcal{A}^{\top} & \mathcal{C}^{\top} \mathcal{C} & 0 & 0 \\ 0 & \mathcal{A} & \mathcal{B} \mathcal{B}^{\top} & \mathcal{B}_0 \\ 0 & 0 & -\mathcal{A}^{\top} & \mathcal{C}_0 \end{array} \right] T^{-1}, \quad T \left[\begin{array}{c} 0 \\ \mathcal{B}_0 \\ \mathcal{C}_0 \end{array} \right], \quad [\mathcal{B}_1 \quad \mathcal{C}_1 \quad 0] T^{-1} \quad (30)$$

with the transformation matrix

$$T = \begin{bmatrix} I & 0 & 0 \\ 0 & I & -\Sigma_{\mathcal{K}} \\ 0 & 0 & I \end{bmatrix},$$

we can get

$$\begin{aligned} & (\mathbf{M}_{12}^{\mathcal{K}}(-s))^{\top} \mathbf{M}_{11}^{\mathcal{K}}(s) (\mathbf{M}_{21}^{\mathcal{K}}(-s))^{\top} \\ &= \left[\begin{array}{ccc|c} -\mathcal{A}^{\top} & \mathcal{C}^{\top} \mathcal{C} & \mathcal{C}^{\top} \mathcal{C} \Sigma_{\mathcal{K}} & 0 \\ 0 & \mathcal{A} & \Sigma_{\mathcal{K}} \mathcal{A}^{\top} + \mathcal{A} \Sigma_{\mathcal{K}} + \mathcal{B} \mathcal{B}^{\top} & \mathcal{B}_0 - \Sigma_{\mathcal{K}} \mathcal{C}_0 \\ 0 & 0 & -\mathcal{A}^{\top} & \mathcal{C}_0 \\ \hline \mathcal{B}_1 & \mathcal{C}_1 & \mathcal{C}_1 \Sigma_{\mathcal{K}} & 0 \end{array} \right], \end{aligned}$$

From Lyapunov equation (12), it follows that $\Sigma_{\mathcal{K}} \mathcal{A}^{\top} + \mathcal{A} \Sigma_{\mathcal{K}} + \mathcal{B} \mathcal{B}^{\top} = 0$. By applying a similar similarity transformation to (29)

$$\begin{aligned} & T' \left[\begin{array}{ccc|c} -\mathcal{A}^{\top} & \mathcal{C}^{\top} \mathcal{C} & \mathcal{C}^{\top} \mathcal{C} \Sigma_{\mathcal{K}} & 0 \\ 0 & \mathcal{A} & \Sigma_{\mathcal{K}} \mathcal{A}^{\top} + \mathcal{A} \Sigma_{\mathcal{K}} + \mathcal{B} \mathcal{B}^{\top} & \mathcal{B}_0 - \Sigma_{\mathcal{K}} \mathcal{C}_0 \\ 0 & 0 & -\mathcal{A}^{\top} & \mathcal{C}_0 \end{array} \right] T'^{-1}, \\ & T' \left[\begin{array}{c} 0 \\ \mathcal{B}_0 - \Sigma_{\mathcal{K}} \mathcal{C}_0 \\ \mathcal{C}_0 \end{array} \right], \quad [\mathcal{B}_1 \quad \mathcal{C}_1 \quad \mathcal{C}_1 \Sigma_{\mathcal{K}}] T'^{-1} \end{aligned} \quad (31)$$

with transformation matrix

$$T' = \begin{bmatrix} I & \mathcal{P}_{\mathcal{K}} & 0 \\ 0 & I & 0 \\ 0 & 0 & I \end{bmatrix},$$

we obtain

$$\begin{aligned} & (\mathbf{M}_{12}^{\mathcal{K}}(-s))^{\top} \mathbf{M}_{11}^{\mathcal{K}}(s) (\mathbf{M}_{21}^{\mathcal{K}}(-s))^{\top} \\ &= \left[\begin{array}{ccc|c} -\mathcal{A}^{\top} & \mathcal{A}^{\top} \mathcal{P}_{\mathcal{K}} + \mathcal{P}_{\mathcal{K}} \mathcal{A} + \mathcal{C}^{\top} \mathcal{C} & \mathcal{C}^{\top} \mathcal{C} \Sigma_{\mathcal{K}} & \mathcal{P}_{\mathcal{K}} (\mathcal{B}_0 - \Sigma_{\mathcal{K}} \mathcal{C}_0) \\ 0 & \mathcal{A} & 0 & \mathcal{B}_0 - \Sigma_{\mathcal{K}} \mathcal{C}_0 \\ 0 & 0 & -\mathcal{A}^{\top} & \mathcal{C}_0 \\ \hline \mathcal{B}_1 & \mathcal{C}_1 - \mathcal{B}_1 \mathcal{P}_{\mathcal{K}} & \mathcal{C}_1 \Sigma_{\mathcal{K}} & 0 \end{array} \right]. \end{aligned}$$

Similarly, Lyapunov equation (12) gives $\mathcal{A}^{\top} \mathcal{P}_{\mathcal{K}} + \mathcal{P}_{\mathcal{K}} \mathcal{A} + \mathcal{C}^{\top} \mathcal{C} = 0$. Consequently, based on the above analysis, the expression $(\mathbf{M}_{12}^{\mathcal{K}}(-s))^{\top} \mathbf{M}_{11}^{\mathcal{K}}(s) (\mathbf{M}_{21}^{\mathcal{K}}(-s))^{\top}$ can be further simplified as

$$\begin{aligned} & (\mathbf{M}_{12}^{\mathcal{K}}(-s))^{\top} \mathbf{M}_{11}^{\mathcal{K}}(s) (\mathbf{M}_{21}^{\mathcal{K}}(-s))^{\top} \\ &= \mathcal{B}_1 (sI + \mathcal{A}^{\top})^{-1} \mathcal{P}_{\mathcal{K}} (\mathcal{B}_0 - \Sigma_{\mathcal{K}} \mathcal{C}_0) + (\mathcal{C}_1 - \mathcal{B}_1 \mathcal{P}_{\mathcal{K}}) (sI - \mathcal{A})^{-1} (\mathcal{B}_0 - \Sigma_{\mathcal{K}} \mathcal{C}_0) \\ & \quad + \mathcal{C}_1 \Sigma_{\mathcal{K}} (sI + \mathcal{A}^{\top})^{-1} \mathcal{C}_0 + \mathcal{B}_1 (sI + \mathcal{A}^{\top})^{-1} \mathcal{C}^{\top} \mathcal{C} \Sigma_{\mathcal{K}} (sI - \mathcal{A})^{-1} \mathcal{C}_0. \end{aligned}$$

Among these terms, only the second term is stable, while the first, third, and fourth terms are anti-stable. Consequently, in light of Lemma 3.3, we conclude that

$$\begin{aligned} & \langle G_{\mathcal{K}}, \Delta G \rangle_{\mathcal{H}_2} \\ &= \text{tr} \left(\int_{-\infty}^{\infty} ((\mathbf{M}_{12}^{\mathcal{K}}(j\omega))^* \mathbf{M}_{11}^{\mathcal{K}}(j\omega) (\mathbf{M}_{21}^{\mathcal{K}}(j\omega))^*) (\Delta \mathcal{K} (I - \mathbf{M}_{22}^{\mathcal{K}}(j\omega) \Delta \mathcal{K})^{-1})^* \frac{d\omega}{2\pi} \right) \end{aligned}$$

$$\begin{aligned}
&= \text{tr} \left(\text{Res}_{\Re(s) \leq 0} (\mathcal{B}_1(sI + \mathcal{A}^\top)^{-1} \mathcal{P}_\mathcal{K} (\mathcal{B}_0 - \Sigma_\mathcal{K} \mathcal{C}_0) (\Delta \mathcal{K} (I - \mathbf{M}_{22}^\mathcal{K}(-s) \Delta \mathcal{K})^{-1})^\top) \right. \\
&\quad + \text{Res}_{\Re(s) \leq 0} ((\mathcal{C}_1 - \mathcal{B}_1 \mathcal{P}_\mathcal{K})(sI - \mathcal{A})^{-1} (\mathcal{B}_0 - \Sigma_\mathcal{K} \mathcal{C}_0) (\Delta \mathcal{K} (I - \mathbf{M}_{22}^\mathcal{K}(-s) \Delta \mathcal{K})^{-1})^\top) \\
&\quad + \text{Res}_{\Re(s) \leq 0} (\mathcal{C}_1 \Sigma_\mathcal{K} (sI + \mathcal{A}^\top)^{-1} \mathcal{C}_0 (\Delta \mathcal{K} (I - \mathbf{M}_{22}^\mathcal{K}(-s) \Delta \mathcal{K})^{-1})^\top) \\
&\quad \left. + \text{Res}_{\Re(s) \leq 0} (\mathcal{B}_1(sI + \mathcal{A}^\top)^{-1} \mathcal{C}^\top \mathcal{C} \Sigma_\mathcal{K} (sI + \mathcal{A}^\top)^{-1} \mathcal{C}_0 (\Delta \mathcal{K} (I - \mathbf{M}_{22}^\mathcal{K}(-s) \Delta \mathcal{K})^{-1})^\top) \right) \\
&= \text{tr} \left(\text{Res}_{\Re(s) \leq 0} ((\mathcal{C}_1 - \mathcal{B}_1 \mathcal{P}_\mathcal{K})(sI - \mathcal{A})^{-1} (\mathcal{B}_0 - \Sigma_\mathcal{K} \mathcal{C}_0) (\Delta \mathcal{K} (I - \mathbf{M}_{22}^\mathcal{K}(-s) \Delta \mathcal{K})^{-1})^\top) \right).
\end{aligned}$$

Therefore, a sufficient condition for $(\mathbf{M}_{12}^\mathcal{K}(-s))^\top \mathbf{M}_{11}^\mathcal{K}(s) (\mathbf{M}_{21}^\mathcal{K}(-s))^\top$ to be anti-stable is that the second term in (3.2) vanishes. The preceding analysis has established the sufficiency of this condition.

We now turn to the necessity part of the proof. For notational consistency and to facilitate subsequent derivations, we recall the definitions introduced earlier in (27), specifically, we have

$$\begin{aligned}
\mathcal{C}_1 - \mathcal{B}_1 \mathcal{P}_\mathcal{K} &= \begin{bmatrix} B^\top P_1^\mathcal{K} + R \bar{C}_\mathcal{K} \\ P_2^\mathcal{K} \end{bmatrix}, \\
\mathcal{B}_0 - \Sigma_\mathcal{K} \mathcal{C}_0 &= [(C \Sigma_1^\mathcal{K})^\top + \bar{B}_\mathcal{K} \mathcal{V} \quad \Sigma_2^{\mathcal{K}\top}],
\end{aligned}$$

where the involved matrices are defined by the following partitions and constructions:

$$\begin{aligned}
P_1^\mathcal{K} &= [P_{11}^\mathcal{K} \quad P_{12}^\mathcal{K}], & P_2^\mathcal{K} &= [P_{21}^\mathcal{K} \quad P_{22}^\mathcal{K}], \\
\Sigma_1^\mathcal{K} &= [\Sigma_{11}^\mathcal{K} \quad \Sigma_{12}^\mathcal{K}], & \Sigma_2^\mathcal{K} &= [\Sigma_{21}^\mathcal{K} \quad \Sigma_{22}^\mathcal{K}], \\
\bar{C}_\mathcal{K} &= [0_{m_1 \times n} \quad C_\mathcal{K}], & \bar{B}_\mathcal{K} &= \begin{bmatrix} 0_{n \times m_2} \\ B_\mathcal{K} \end{bmatrix}.
\end{aligned} \tag{32}$$

Suppose that \mathcal{K} is an optimal solution to problem (8). The term $(\mathcal{C}_1 - \mathcal{B}_1 \mathcal{P}_\mathcal{K})(sI - \mathcal{A})^{-1} (\mathcal{B}_0 - \Sigma_\mathcal{K} \mathcal{C}_0)$ admits the following block expansion:

$$\begin{aligned}
&\begin{bmatrix} B^\top P_1^\mathcal{K} + R \bar{C}_\mathcal{K} \\ P_2^\mathcal{K} \end{bmatrix} (sI - \mathcal{A})^{-1} [(C \Sigma_1^\mathcal{K})^\top + \bar{B}_\mathcal{K} \mathcal{V} \quad \Sigma_2^{\mathcal{K}\top}] \\
&= \begin{bmatrix} (B^\top P_1^\mathcal{K} + R \bar{C}_\mathcal{K})(sI - \mathcal{A})^{-1} ((C \Sigma_1^\mathcal{K})^\top + \bar{B}_\mathcal{K} \mathcal{V}) & (B^\top P_1^\mathcal{K} + R \bar{C}_\mathcal{K})(sI - \mathcal{A})^{-1} \Sigma_2^{\mathcal{K}\top} \\ P_2^\mathcal{K} (sI - \mathcal{A})^{-1} ((C \Sigma_1^\mathcal{K})^\top + \bar{B}_\mathcal{K} \mathcal{V}) & P_2^\mathcal{K} (sI - \mathcal{A})^{-1} \Sigma_2^{\mathcal{K}\top} \end{bmatrix},
\end{aligned}$$

According to Theorem 2 in [41], any optimal solution must satisfy

$$(B^\top P_1^\mathcal{K} + R \bar{C}_\mathcal{K})(sI - \mathcal{A})^{-1} ((C \Sigma_1^\mathcal{K})^\top + \bar{B}_\mathcal{K} \mathcal{V}) \equiv 0.$$

This condition ensures that the leading block of (27) vanishes. Consequently, it remains to analyze the remaining terms. Assume that $\omega_0 \in \mathbb{R}$ makes $(\mathcal{C}_1 - \mathcal{B}_1 \mathcal{P}_\mathcal{K})(j\omega_0 I - \mathcal{A})^{-1} (\mathcal{B}_0 - \Sigma_\mathcal{K} \mathcal{C}_0) \neq 0$. Then, we can consider a stable transfer function $\hat{\mathcal{F}}(s)$

$$\begin{aligned}
\hat{\mathcal{F}}(s) &= \begin{bmatrix} 0 & (B^\top P_1^\mathcal{K} + R \bar{C}_\mathcal{K})(sI - \mathcal{A})^{-1} \Sigma_2^{\mathcal{K}\top} \\ P_2^\mathcal{K} (sI - \mathcal{A})^{-1} ((C \Sigma_1^\mathcal{K})^\top + \bar{B}_\mathcal{K} \mathcal{V}) & P_2^\mathcal{K} (sI - \mathcal{A})^{-1} \Sigma_2^{\mathcal{K}\top} \end{bmatrix} \\
&= \begin{bmatrix} \hat{\mathcal{F}}_{11}(s) & \hat{\mathcal{F}}_{12}(s) \\ \hat{\mathcal{F}}_{21}(s) & \hat{\mathcal{F}}_{22}(s) \end{bmatrix}.
\end{aligned}$$

By the bijectivity of Youla parametrization, there exists a perturbation $\Delta \mathcal{K}$ such that $\Delta \mathcal{K} (I - \mathbf{M}_{22}^\mathcal{K}(s) \Delta \mathcal{K})^{-1} = \epsilon \hat{\mathcal{F}}(s)$ for some constant $\epsilon < 0$.

Under these settings, the integral of the coupling term

$$\text{tr} \left(\int_{-\infty}^{\infty} ((\mathbf{M}_{12}^\mathcal{K}(j\omega))^* \mathbf{M}_{11}^\mathcal{K}(j\omega) (\mathbf{M}_{21}^\mathcal{K}(j\omega))^*) (\Delta \mathcal{K} (I - \mathbf{M}_{22}^\mathcal{K}(j\omega) \Delta \mathcal{K})^{-1})^* \frac{d\omega}{2\pi} \right)$$

becomes

$$\epsilon \int_{-\infty}^{\infty} \text{tr} \left(\hat{\mathcal{F}}_{12}(j\omega) (\hat{\mathcal{F}}_{12}(j\omega))^* + \hat{\mathcal{F}}_{21}(j\omega) (\hat{\mathcal{F}}_{21}(j\omega))^* + \hat{\mathcal{F}}_{22}(j\omega) (\hat{\mathcal{F}}_{22}(j\omega))^* \right) \frac{d\omega}{2\pi} = \epsilon \|\hat{\mathcal{F}}\|_{\mathcal{H}_2}^2.$$

We prove necessity by contradiction. Assume the condition (57) does not hold, meaning the corresponding stable transfer function is not identically zero. By the Maximum Modulus Principle, this function must be non-zero on the imaginary axis, which implies that our constructed $\hat{\mathcal{F}}(s)$ is non-zero and its \mathcal{H}_2 norm is strictly positive ($\|\hat{\mathcal{F}}\|_{\mathcal{H}_2}^2 > 0$). The first-order change in cost is then $\epsilon \|\hat{\mathcal{F}}\|_{\mathcal{H}_2}^2$. Choosing $\epsilon < 0$ leads to a cost decrease, which contradicts the assumed optimality of \mathcal{K} . Thus, the condition (57) must hold. \square

Remark 3.5. We present an equivalent algebraic formulation in the state-space domain to gain further insight into the optimality condition (27). This reformulation transforms the original infinite-dimensional frequency-domain condition (27) into a set of finite-dimensional equations, thereby providing a complementary perspective and facilitating the analysis of the structural properties of optimal solutions of problem (8).

Standard results in state-space theory imply that the optimality condition (27) holds if and only if the following system is anti-stable:

$$\left[\begin{array}{c|c} \mathcal{A} & \mathcal{B}_0 - \Sigma_{\mathcal{K}} \mathcal{C}_0 \\ \hline \mathcal{C}_1 - \mathcal{B}_1 \mathcal{P}_{\mathcal{K}} & 0 \end{array} \right]. \quad (33)$$

Moreover, under the assumption that \mathcal{A} is stable, standard definitions of controllability and observability imply that system (33) is anti-stable if and only if its Kalman decomposition contains no subsystem that is both controllable and observable. It is equivalent to

$$(\mathcal{C}_1 - \mathcal{B}_1 \mathcal{P}_{\mathcal{K}}) \mathcal{A}^i (\mathcal{B}_0 - \Sigma_{\mathcal{K}} \mathcal{C}_0) = 0, \quad \forall i = 0, 1, \dots, n + q - 1. \quad (34)$$

This algebraic formulation enables the derivation of more tractable sufficient conditions for optimality, thereby facilitating the analysis and design of practical algorithms. For example, the following corollary presents a sufficient condition that generalizes the optimality results in [35].

Corollary 3.6. *A controller parameter \mathcal{K} is globally optimal for LQG (or \mathcal{H}_2) problem if*

1. \mathcal{K} is a stationary point of problem (8): $\nabla J(\mathcal{K}) = 0$.
2. The rank condition $\text{rank} \begin{pmatrix} P_{21}^{\mathcal{K}} & P_{22}^{\mathcal{K}} \end{pmatrix} = \text{rank} \begin{pmatrix} \Sigma_{21}^{\mathcal{K}} & \Sigma_{22}^{\mathcal{K}} \end{pmatrix} = q$ holds.

Proof. The gradient components of cost functional with respect to the three controller parameters, $A_{\mathcal{K}}$, $B_{\mathcal{K}}$, and $C_{\mathcal{K}}$, are given by

$$\nabla_{A_{\mathcal{K}}} J(\mathcal{K}) = 2(P_2^{\mathcal{K}} \Sigma_2^{\mathcal{K}\top}), \quad (35)$$

$$\nabla_{B_{\mathcal{K}}} J(\mathcal{K}) = 2(P_{22}^{\mathcal{K}} B_{\mathcal{K}} \mathcal{V} + P_2^{\mathcal{K}} \Sigma_1^{\mathcal{K}\top} C^{\top}), \quad (36)$$

$$\nabla_{C_{\mathcal{K}}} J(\mathcal{K}) = 2(R C_{\mathcal{K}} \Sigma_{22}^{\mathcal{K}} + B^{\top} P_1^{\mathcal{K}} \Sigma_2^{\mathcal{K}\top}), \quad (37)$$

where the matrices $P_1^{\mathcal{K}}$, $P_2^{\mathcal{K}}$, $\Sigma_1^{\mathcal{K}}$ and $\Sigma_2^{\mathcal{K}}$ are defined in (32).

Next, we utilize Lyapunov equation (12), which plays a key role in establishing the relationships among the relevant variables. In particular, we compute

$$\begin{aligned} \mathcal{P}_{\mathcal{K}} \mathcal{A} \Sigma_2^{\mathcal{K}\top} + \mathcal{A}^{\top} \mathcal{P}_{\mathcal{K}} \Sigma_2^{\mathcal{K}\top} &= \begin{bmatrix} P_1^{\mathcal{K}} \mathcal{A} \Sigma_2^{\mathcal{K}\top} \\ P_2^{\mathcal{K}} \mathcal{A} \Sigma_2^{\mathcal{K}\top} \end{bmatrix} + \mathcal{A}^{\top} \begin{bmatrix} P_1^{\mathcal{K}} \Sigma_2^{\mathcal{K}\top} \\ P_2^{\mathcal{K}} \Sigma_2^{\mathcal{K}\top} \end{bmatrix} \\ &\stackrel{(35)}{=} \begin{bmatrix} P_1^{\mathcal{K}} \mathcal{A} \Sigma_2^{\mathcal{K}\top} \\ P_2^{\mathcal{K}} \mathcal{A} \Sigma_2^{\mathcal{K}\top} \end{bmatrix} + \mathcal{A}^{\top} \begin{bmatrix} P_1^{\mathcal{K}} \Sigma_2^{\mathcal{K}\top} \\ 0 \end{bmatrix} \\ &= \begin{bmatrix} P_1^{\mathcal{K}} \mathcal{A} \Sigma_2^{\mathcal{K}\top} \\ P_2^{\mathcal{K}} \mathcal{A} \Sigma_2^{\mathcal{K}\top} \end{bmatrix} + \begin{bmatrix} A_{\mathcal{K}}^{\top} P_1^{\mathcal{K}} \Sigma_2^{\mathcal{K}\top} \\ C_{\mathcal{K}}^{\top} B^{\top} P_1^{\mathcal{K}} \Sigma_2^{\mathcal{K}\top} \end{bmatrix} \\ &\stackrel{(12)}{=} - \begin{bmatrix} Q \Sigma_{12}^{\mathcal{K}} \\ C_{\mathcal{K}}^{\top} R C_{\mathcal{K}} \Sigma_{22}^{\mathcal{K}} \end{bmatrix}. \end{aligned}$$

Finally, by invoking the stationarity condition for $C_{\mathcal{K}}$ (37), we obtain

$$\begin{bmatrix} P_1^{\mathcal{K}} \mathcal{A} \Sigma_2^{\mathcal{K}\top} \\ P_2^{\mathcal{K}} \mathcal{A} \Sigma_2^{\mathcal{K}\top} \end{bmatrix} + \begin{bmatrix} A_{\mathcal{K}}^{\top} P_1^{\mathcal{K}} \Sigma_2^{\mathcal{K}\top} \\ C_{\mathcal{K}}^{\top} \frac{\nabla_{C_{\mathcal{K}}} J(\mathcal{K})}{2} \end{bmatrix} = \begin{bmatrix} P_1^{\mathcal{K}} \mathcal{A} \Sigma_2^{\mathcal{K}\top} \\ P_2^{\mathcal{K}} \mathcal{A} \Sigma_2^{\mathcal{K}\top} \end{bmatrix} + \begin{bmatrix} A_{\mathcal{K}}^{\top} P_1^{\mathcal{K}} \Sigma_2^{\mathcal{K}\top} \\ 0 \end{bmatrix} = - \begin{bmatrix} Q \Sigma_{12}^{\mathcal{K}} \\ 0 \end{bmatrix}.$$

Focusing on the lower block of the above equation, we obtain the following key relationship

$$P_2^{\mathcal{K}} \mathcal{A} \Sigma_2^{\mathcal{K}\top} = 0. \quad (38)$$

To further exploit this structure, we construct a transformation matrix based on the rank condition $\text{rank}(\Sigma_2^{\mathcal{K}}) = \text{rank}(P_2^{\mathcal{K}}) = q$. Specifically, let

$$U = \begin{bmatrix} (\Sigma_2^{\mathcal{K}} \Sigma_2^{\mathcal{K}\top})^{-1} \Sigma_2^{\mathcal{K}} \\ P_2^{\mathcal{K}} \end{bmatrix}, \quad U^{-1} = \begin{bmatrix} \Sigma_2^{\mathcal{K}\top} & P_2^{\mathcal{K}\top} (P_2^{\mathcal{K}} P_2^{\mathcal{K}\top})^{-1} \end{bmatrix};$$

applying this transformation matrix to the transfer function (27), we obtain

$$\begin{aligned}
& (\mathcal{C}_1 - \mathcal{B}_1 \mathcal{P}_\mathcal{K})(sI - \mathcal{A})^{-1}(\mathcal{B}_0 - \Sigma_\mathcal{K} \mathcal{C}_0) \\
&= (\mathcal{C}_1 - \mathcal{B}_1 \mathcal{P}_\mathcal{K})U^{-1}U(sI - \mathcal{A})U^{-1}U(\mathcal{B}_0 - \Sigma_\mathcal{K} \mathcal{C}_0) \\
&= [\alpha \quad \beta] \left(sI - \begin{bmatrix} * & * \\ 0 & * \end{bmatrix} \right)^{-1} \begin{bmatrix} \gamma \\ \delta \end{bmatrix}, \tag{39}
\end{aligned}$$

where the block upper triangular structure of the transformed system matrix follows directly from (38). Compute the components

$$\gamma = (\Sigma_2^\mathcal{K} \Sigma_2^{\mathcal{K}\top})^{-1} \Sigma_2^\mathcal{K} (\mathcal{B}_0 - \Sigma_\mathcal{K} \mathcal{C}_0) = [(\Sigma_2^\mathcal{K} \Sigma_2^{\mathcal{K}\top})^{-1} \Sigma_2^\mathcal{K} ((C \Sigma_1^\mathcal{K})^\top + \bar{B}_\mathcal{K} \mathcal{V}) \quad I], \tag{40}$$

$$\delta = P_2^\mathcal{K} (\mathcal{B}_0 - \Sigma_\mathcal{K} \mathcal{C}_0) = \begin{bmatrix} P_2^\mathcal{K} \Sigma_1^\mathcal{K} C^\top + P_2^\mathcal{K} \bar{B}_\mathcal{K} \mathcal{V} \\ P_2^\mathcal{K} \Sigma_2^{\mathcal{K}\top} \end{bmatrix} = 0, \quad (\text{by (35) and (36)}) \tag{41}$$

$$\alpha = (\mathcal{C}_1 - \mathcal{B}_1 \mathcal{P}_\mathcal{K}) \Sigma_2^{\mathcal{K}\top} = \begin{bmatrix} P_2^\mathcal{K} \Sigma_2^{\mathcal{K}\top} \\ (B^\top P_1^\mathcal{K} + R \bar{C}_\mathcal{K}) \Sigma_2^{\mathcal{K}\top} \end{bmatrix} = 0 \quad (\text{by (35) and (37)}), \tag{42}$$

$$\beta = (\mathcal{C}_1 - \mathcal{B}_1 \mathcal{P}_\mathcal{K}) P_2^{\mathcal{K}\top} (P_2^\mathcal{K} P_2^{\mathcal{K}\top})^{-1} = \begin{bmatrix} (B^\top P_1^\mathcal{K} + R \bar{C}_\mathcal{K}) P_2^{\mathcal{K}\top} (P_2^\mathcal{K} P_2^{\mathcal{K}\top})^{-1} \\ I \end{bmatrix}. \tag{43}$$

Substituting (40)-(43) into (39) shows the expression $(\mathcal{C}_1 - \mathcal{B}_1 \mathcal{P}_\mathcal{K})(sI - \mathcal{A})^{-1}(\mathcal{B}_0 - \Sigma_\mathcal{K} \mathcal{C}_0) = 0$. By Theorem 3.4, \mathcal{K} is globally optimal. \square

4 The difference of optimality conditions of LQG and LQR

In this section, we present our second main contribution: a structural explanation for the existence of suboptimal stationary points in LQG problem. It is well-known that stationary points of LQG problem (8) are not necessarily globally optimal [30]. Our frequency-domain criterion, established in Theorem 3.4, provides the precise tool to analyze this phenomenon. Specifically, a stationary point is optimal if and only if the optimality condition

$$(\mathcal{C}_1 - \mathcal{B}_1 \mathcal{P}_\mathcal{K})(sI - \mathcal{A})^{-1}(\mathcal{B}_0 - \Sigma_\mathcal{K} \mathcal{C}_0) \equiv 0, \quad \forall s \in \mathbb{C}$$

is satisfied. This issue stands in stark contrast to the classic LQR problem, which is well-behaved in that its unique stationary point is always globally optimal.

To illuminate this fundamental discrepancy, we will now dissect the structural differences between the LQG and LQR optimization landscapes. We begin by recalling LQR problem with a state-feedback gain K :

$$\begin{aligned}
\min_{K \in \mathbb{K}_{LQR}} \quad & f_{LQR}(K) := \lim_{T \rightarrow \infty} \frac{1}{T} \mathbb{E} \left[\int_0^T (x_t^\top Q x_t + u_t^\top R u_t) dt \right], \\
\text{s.t.} \quad & \begin{cases} \dot{x}_t = A x_t + B u_t + \omega'_t, \\ y_t = x_t, \quad (\text{full state measurement}) \\ u_t = K y_t, \end{cases} \tag{44}
\end{aligned}$$

where \mathbb{K}_{LQR} denotes the set of all the state-feedback gains that stabilize system (44), and $\{\omega'_t\}$ is the Gaussian white noise process with intensity matrix I ; the remaining notation is consistent with that in (4).

Definition. A stationary point for LQR problem (44) is any feedback gain K that satisfies

$$\nabla_K f_{LQR}(K) = 0. \tag{45}$$

To illustrate the explanatory power of our framework, we now use it to deconstruct the well-known difference between the LQR and LQG optimization landscapes. We begin with the LQR case. Unlike the general LQG problem, problem (44) is known to admit a unique stationary point, which is also globally optimal [9]. The following theorem formalizes the insight gained from our framework (Theorem 3.4): it demonstrates that the structure of LQR problem is precisely what forces any stationary point to satisfy

the global optimality condition. This perspective not only recovers the classic result but also sets the stage for our subsequent analysis in Remark 4.2, which will pinpoint exactly why suboptimal stationary points arise in the more challenging LQG setting.

Theorem 4.1. *There exists a unique stationary point of problem (44), and it is the global optimum.*

Proof. To analyze the stationary points of problem (44), we examine how the cost functional changes when the feedback gain is perturbed. Specifically, for any $K \in \mathbb{K}_{LQR}$, we consider a small perturbation ΔK such that the new controller $K' = K + \Delta K$ also belongs to \mathbb{K}_{LQR} . The corresponding closed-loop system of problem (44) under K' is given by

$$\dot{x}_t = Ax_t + Bu_t + \omega'_t, \quad u_t = K'x_t = Kx_t + \Delta Kx_t. \quad (46)$$

As in the LQG case (see the proof of Lemma 3.2 and Eqs. (19)–(24) there), the LQR performance functional $f_{LQR}(K')$ can also be represented as the square of a \mathcal{H}_2 norm:

$$f_{LQR}(K') = \|\mathbf{M}_{11}^K + \mathbf{M}_{12}^K \Delta K (I - \mathbf{M}_{22}^K \Delta K)^{-1} \mathbf{M}_{21}^K\|_{\mathcal{H}_2}^2 \quad (47)$$

with transfer matrices

$$\begin{aligned} \mathbf{M}_{11}^K(s) &= \begin{bmatrix} Q^{1/2} \\ R^{1/2}K \end{bmatrix} (sI - (A + BK))^{-1}, \\ \mathbf{M}_{12}^K(s) &= \begin{bmatrix} Q^{1/2} \\ R^{1/2}K \end{bmatrix} (sI - (A + BK))^{-1}B + \begin{bmatrix} 0 \\ R^{1/2} \end{bmatrix}, \\ \mathbf{M}_{21}^K(s) &= (sI - (A + BK))^{-1}, \\ \mathbf{M}_{22}^K(s) &= (sI - (A + BK))^{-1}B. \end{aligned} \quad (48)$$

As shown in (48), the squared \mathcal{H}_2 norm in (47) can be expanded as

$$\begin{aligned} &\|\mathbf{M}_{11}^K\|_{\mathcal{H}_2}^2 + \|\mathbf{M}_{12}^K \Delta K (I - \mathbf{M}_{22}^K \Delta K)^{-1} \mathbf{M}_{21}^K\|_{\mathcal{H}_2}^2 \\ &+ 2 \langle \mathbf{M}_{11}^K, \mathbf{M}_{12}^K \Delta K (I - \mathbf{M}_{22}^K \Delta K)^{-1} \mathbf{M}_{21}^K \rangle_{\mathcal{H}_2}. \end{aligned} \quad (49)$$

For the stationary point analysis, recall that—as in (26)—a sufficient optimality condition is

$$\langle \mathbf{M}_{11}^K, \mathbf{M}_{12}^K \Delta K (I - \mathbf{M}_{22}^K \Delta K)^{-1} \mathbf{M}_{21}^K \rangle_{\mathcal{H}_2} = 0 \quad (50)$$

for all the admissible ΔK . According to Lemma 3.3, (50) occurs precisely when the matrix-function

$$(\mathbf{M}_{12}^K(-s))^\top \mathbf{M}_{11}^K(s) (\mathbf{M}_{21}^K(-s))^\top$$

is anti-stable, i.e., it has no nontrivial zeros in the closed right half-plane.

To connect the condition of anti-stable to the system matrices, we explicitly construct a state-space realization for $(\mathbf{M}_{12}^K(-s))^\top \mathbf{M}_{11}^K(s) (\mathbf{M}_{21}^K(-s))^\top$:

$$\begin{aligned} &(\mathbf{M}_{12}^K(-s))^\top \mathbf{M}_{11}^K(s) (\mathbf{M}_{21}^K(-s))^\top \\ &= \left[\begin{array}{ccc|c} -(A + BK)^\top & Q + K^\top RK & 0 & 0 \\ 0 & A + BK & I & 0 \\ 0 & 0 & -(A + BK)^\top & I \\ \hline B^\top & RK & 0 & 0 \end{array} \right]. \end{aligned} \quad (51)$$

This realization highlights the connection between the system dynamics under K and the instability condition.

Following the proof of Theorem 3.4, we introduce the transformation matrices

$$T = \begin{bmatrix} I & 0 & 0 \\ 0 & I & -\Sigma_K \\ 0 & 0 & I \end{bmatrix} \quad \text{and} \quad T' = \begin{bmatrix} I & P_K & 0 \\ 0 & I & 0 \\ 0 & 0 & I \end{bmatrix},$$

where P_K and Σ_K solve the Lyapunov equations

$$\begin{aligned} (A + BK)^\top P_K + P_K(A + BK) &= -(Q + K^\top RK), \\ (A + BK)\Sigma_K + \Sigma_K(A + BK)^\top &= -I. \end{aligned} \quad (52)$$

Applying a similarity transformation with the composite matrix $T'T$ to the system matrices in (51)

$$\begin{aligned} T'T \begin{bmatrix} -(A + BK)^\top & Q + K^\top RK & 0 \\ 0 & A + BK & I \\ 0 & 0 & -(A + BK)^\top \end{bmatrix} (TT')^{-1}, \\ TT' \begin{bmatrix} 0 \\ 0 \\ I \end{bmatrix}, \quad [B^\top \quad RK \quad 0] (TT')^{-1} \end{aligned} \quad (53)$$

respectively, yields the transformed realization:

$$\begin{aligned} &(\mathbf{M}_{12}^K(-s))^\top \mathbf{M}_{11}^K(s) (\mathbf{M}_{21}^K(-s))^\top \\ &= \left[\begin{array}{ccc|c} -(A + BK)^\top & 0 & (Q + K^\top RK)\Sigma_K & P_K\Sigma_K \\ 0 & (A + BK) & 0 & -\Sigma_K \\ 0 & 0 & -(A + BK)^\top & I \\ \hline B^\top & -BP_K + RK & RK\Sigma_K & 0 \end{array} \right], \end{aligned} \quad (54)$$

Based on (54), we can decompose $(\mathbf{M}_{12}^K(-s))^\top \mathbf{M}_{11}^K(s) (\mathbf{M}_{21}^K(-s))^\top$ into four subsystems:

$$\begin{aligned} &(\mathbf{M}_{12}^K(-s))^\top \mathbf{M}_{11}^K(s) (\mathbf{M}_{21}^K(-s))^\top \\ &= B^\top (sI + (A + BK)^\top)^{-1} P_K \Sigma_K + RK \Sigma_K (sI + (A + BK)^\top)^{-1} \\ &\quad + B^\top (sI + (A + BK)^\top)^{-1} (Q + K^\top RK) \Sigma_K (sI + (A + BK)^\top)^{-1} \\ &\quad - (-BP_K + RK) (sI - (A + BK))^{-1} \Sigma_K. \end{aligned} \quad (55)$$

It is straightforward to verify that, among these terms, only the last term is stable, as it is associated with the stable part of the closed-loop dynamics.

Substituting the above decomposition into the cross-term $\langle \mathbf{M}_{11}^K, \mathbf{M}_{12}^K \Delta K (I - \mathbf{M}_{22}^K \Delta K)^{-1} \mathbf{M}_{21}^K \rangle_{\mathcal{H}_2}$, we obtain

$$\begin{aligned} &\langle \mathbf{M}_{11}^K, \mathbf{M}_{12}^K \Delta K (I - \mathbf{M}_{22}^K \Delta K)^{-1} \mathbf{M}_{21}^K \rangle_{\mathcal{H}_2} \\ &= \text{tr} \left(\int_{-\infty}^{\infty} \mathbf{M}_{12}^K(j\omega)^* \mathbf{M}_{11}^K(j\omega) \mathbf{M}_{21}^K(j\omega)^* (\Delta K (I - \mathbf{M}_{22}^K(j\omega) \Delta K)^{-1})^* \frac{d\omega}{2\pi} \right) \\ &= \text{tr} \left(\text{Res}_{\Re(s) \leq 0} \left((-BP_K + RK) (sI - (A + BK))^{-1} \Sigma_K (\Delta K (I - \mathbf{M}_{22}^K(-s) \Delta K)^{-1})^\top \right) \right) \\ &= \text{tr} \left(\text{Res}_{\Re(s) \leq 0} \left((-BP_K + RK) (sI - (A + BK))^{-1} \Sigma_K \Delta K^\top \right) \right) + o(\|\Delta K\|) \\ &= \frac{1}{2} \text{tr} (\nabla_K f_{LQR}(K) \Delta K^\top) + o(\|\Delta K\|), \end{aligned} \quad (56)$$

where the last equality holds because

$$\Delta K (I - \mathbf{M}_{22}^K(s) \Delta K)^{-1} = \Delta K + \Delta K (I - (I - \mathbf{M}_{22}^K(s) \Delta K)^{-1})$$

and

$$\|\mathbf{M}_{12}^K \Delta K (I - \mathbf{M}_{22}^K \Delta K)^{-1} \mathbf{M}_{21}^K\|_{\mathcal{H}_2}^2 = o(\|\Delta K\|).$$

Meanwhile, by following the argument in the proof of Theorem 3.4, we establish that K is the optimal solution to problem (44) if and only if

$$(-BP_K + RK) (sI - (A + BK))^{-1} \Sigma_K \equiv 0, \quad \forall s \in \mathbb{C}. \quad (57)$$

Comparing (56) and (57), we observe that the stationary point condition $\nabla_K f_{LQR}(K) = 0$ and the optimality condition for problem (44) coincide. Specifically, we have

$$\begin{aligned} \nabla_K f_{LQR}(K) &= 2 \text{Res}_{\Re(s) \leq 0} \left((-BP_K + RK) (sI - (A + BK))^{-1} \Sigma_K \right) \\ &= 2(-BP_K + RK) \Sigma_K. \end{aligned} \quad (58)$$

Equation (58) shows that the gradient of (44) with respect to K is precisely the residue associated with the optimality condition in (56). Since $\Sigma_K \succ 0$, the transfer function in (56) is absolutely controllable. Therefore, (56) (and hence the gradient) vanishes if and only if $(-BP_K + RK)\Sigma_K = 0$, i.e., the system in (56) is absolutely unobservable. Consequently, all the stationary points of problem (44) correspond to the optimal solutions. Moreover, the unique solution is characterized by $-BP_K + RK = 0$ together with the Lyapunov equation (52), which completes the proof. \square

Remark 4.2. In the LQR problem, the stationarity condition, $\nabla_K f_{\text{LQR}}(K) = 0$, is equivalent to the global optimality condition given by the frequency-domain identity in (57). This equivalence is a special property of the LQR problem's structure.

For the general LQG problem, this equivalence no longer holds. The condition for stationarity, $\nabla J(\mathcal{K}) = 0$, is necessary for optimality but generally not sufficient. This gap between stationarity and optimality can be attributed to two distinct structural properties of the LQG problem.

First, the gradient $\nabla J(\mathcal{K})$ is not equal to the residue itself. The gradient is obtained by projecting the residue onto the subspace of structurally admissible controllers ($\mathbb{K}_q \subseteq \mathbb{R}^{(q+m_1) \times (q+m_2) | m_1 \times m_2}$). This relationship is formalized by:

$$\nabla J(\mathcal{K}) = 2\mathbf{e}_{(q+m_1) \times (q+m_2)}(\text{Res}_{\Re(s) \leq 0}((\mathcal{C}_1 - \mathcal{B}_1 \mathcal{P}_{\mathcal{K}})(sI - \mathcal{A})^{-1}(\mathcal{B}_0 - \Sigma_{\mathcal{K}} \mathcal{C}_0)), m_1, m_2), \quad (59)$$

where $\mathbf{e}(\cdot)$ is the projection operator. This projection is the source of the first gap: the gradient can be zero even if the residue is non-zero, provided the residue is orthogonal to the subspace of admissible controller structures.

Second, a zero residue is a weaker condition than global optimality. The global optimality condition requires the full transfer function to be identically zero for all frequencies:

$$(\mathcal{C}_1 - \mathcal{B}_1 \mathcal{P}_{\mathcal{K}})(sI - \mathcal{A})^{-1}(\mathcal{B}_0 - \Sigma_{\mathcal{K}} \mathcal{C}_0) \equiv 0, \quad \forall s \in \mathbb{C}. \quad (60)$$

Unlike the LQR case, the system underlying the LQG problem is generally not absolutely controllable or observable. As a consequence, the vanishing of the residue is not sufficient to ensure that the transfer function in (60) is identically zero.

In summary, two distinct logical steps separate stationarity from global optimality in the LQG problem: (i) the gradient can be zero without the residue being zero (due to controller structure), and (ii) the residue can be zero without the transfer function being identically zero. These two factors explain why stationary points that are not globally optimal can exist in the LQG optimization landscape.

5 Optimization method based on the optimality condition

In the previous section, we identified a fundamental structural flaw in the direct parameterization (9) of LQG problem. As detailed in Remark 4.2, essential frequency-domain information required for global optimality is lost in the gradients of traditional, direct parameterizations (9). This is not merely a theoretical curiosity; it directly explains why popular gradient-based methods can be trapped at suboptimal points in the LQG setting [30, 41].

To overcome this limitation, this section develops a new controller synthesis framework that preserves this critical information. Our approach is built upon the Youla parameterization, a central tool that recasts the original non-convex synthesis problem into a convex optimization over an infinite-dimensional space of stable transfer functions (the Youla parameter) [17]. Crucially, rather than approximating this problem as a finite-dimensional one, a step that introduces its own unavoidable errors, we design a gradient method that operates directly on this function space. By working in this infinite-dimensional setting, the Fréchet-gradient-based algorithm we developed retains the full frequency-domain structure of the problem. This allows us to establish the global convergence guarantees, thereby addressing the principal weaknesses of existing methods. Our analysis in this section proceeds under the standard assumption that all the system parameters (\mathcal{A} , \mathcal{B}_1 , \mathcal{C}_1 , \mathcal{B}_0 , \mathcal{C}_0 , $\mathcal{P}_{\mathcal{K}}$, and $\Sigma_{\mathcal{K}}$) are known.

5.1 Optimization over the Space \mathcal{RH}_∞

To overcome the limitations of feasible set in problem (8) and recover the frequency-domain information in optimality condition (27), we consider controllers in an infinite-dimensional function space. Specifically, given a fixed initial controller $\mathcal{K} \in \mathbb{K}_q$, we define an enlarged controller set \mathbb{K} , consisting of all the elements of form $\Delta\mathcal{K} = \tilde{\mathcal{K}} - \mathcal{K}$ for $\tilde{\mathcal{K}} \in \mathbb{K}_q$, a translated copy of \mathbb{K}_q centered at \mathcal{K} . More precisely,

$$\mathbb{K} := \left\{ \Delta\mathcal{K}_1(s) + \Delta\mathcal{K}_2 \left| \begin{array}{l} \Delta\mathcal{K}_1(s) \in \mathcal{RH}_{\infty,0}^{(m_1+q) \times (q+m_2)} \cup \{0_{(m_1+q) \times (q+m_2)}\}, \\ \Delta\mathcal{K}_2 \in \mathbb{R}^{(q+m_1) \times (q+m_2) | m_1 \times m_2}, \\ ((\Delta\mathcal{K}_1(s) + \Delta\mathcal{K}_2)(I - \mathbf{M}_{22}^{\mathcal{K}}(\Delta\mathcal{K}_1(s) + \Delta\mathcal{K}_2))^{-1}) \text{ is stable} \end{array} \right. \right\}, \quad (61)$$

where $\mathcal{RH}_{\infty,0}^{(m_1+q) \times (q+m_2)}$ denotes the subset of $\mathcal{RH}_{\infty,0}$ consisting of transfer matrices with m_1+q outputs and $q+m_2$ inputs. This expanded set provides a broader search space for controller synthesis, potentially admitting novel solutions outside the original finite-dimensional set \mathbb{K}_q . Importantly, as seen from (22), for any $\mathcal{K}' \in \mathbb{K}_q$, the difference $\Delta\mathbf{K} = \mathcal{K}' - \mathcal{K}$ satisfies $\Delta\mathbf{K} \in \mathbb{K}$. Therefore, the translated copy of \mathbb{K}_q , given by $\{\mathcal{K}' - \mathcal{K} \mid \mathcal{K}' \in \mathbb{K}_q\}$, is included in the expanded set \mathbb{K} . As a result, the classic optimal LQG controller (as defined in (6)) is still attained—up to translation—within the enlarged optimization domain, and thus the optimal value of the expanded problem coincides with that of the original problem (8).

If we directly substitute $\Delta\mathbf{K} \in \mathbb{K}$ into the original performance criterion as in problem (15),

$$J_{\mathcal{K}}(\Delta\mathbf{K}) = \|\mathbf{M}_{11}^{\mathcal{K}} + \mathbf{M}_{12}^{\mathcal{K}}\Delta\mathbf{K}(I - \mathbf{M}_{22}^{\mathcal{K}}\Delta\mathbf{K})^{-1}\mathbf{M}_{21}^{\mathcal{K}}\|_{\mathcal{H}_2}^2,$$

which leads to a nonconvex optimization problem in $\Delta\mathbf{K}$. To resolve this, we use the Youla parameterization to reformulate the controller in \mathbb{K} , resulting in a convex problem in a new parameter space. For any $\Delta\mathbf{K} \in \mathbb{K}$ and a fixed initial controller $\mathcal{K} \in \mathbb{K}_q$, there exists a unique pair (\mathbf{Q}, Q) in the set \mathbb{U} such that

$$\Delta\mathbf{K}(I - \mathbf{M}_{22}^{\mathcal{K}}\Delta\mathbf{K})^{-1} = \mathbf{Q} + Q,$$

where the set \mathbb{U} is defined as

$$\mathbb{U} := \left\{ (\mathbf{Q}(s), Q) \left| \begin{array}{l} \mathbf{Q}(s) \in \mathcal{RH}_{\infty,0}^{(m_1+q) \times (q+m_2)} \cup \{0_{q+m_1 \times (q+m_2)}\}, \\ Q \in \mathbb{R}^{(q+m_1) \times (q+m_2) | m_1 \times m_2} \cup \{0_{(q+m_1) \times (q+m_2)}\} \end{array} \right. \right\}. \quad (62)$$

The following lemma formalizes the above one-to-one correspondence.

Lemma 5.1. *Let $\mathcal{K} \in \mathbb{K}_q$, and $\forall \Delta\mathbf{K} \in \mathbb{K}$. Then, the following assertions hold*

1. *there exists a unique element $(\mathbf{Q}(\Delta\mathbf{K}), Q(\Delta\mathbf{K})) \in \mathbb{U}$ such that $\Delta\mathbf{K}(I - \mathbf{M}_{22}^{\mathcal{K}}\Delta\mathbf{K})^{-1} = \mathbf{Q}(\Delta\mathbf{K}) + Q(\Delta\mathbf{K})$.*
2. *Conversely, for any $(\mathbf{Q}, Q) \in \mathbb{U}$, there exists a unique $\Delta\mathbf{K} \in \mathbb{K}$ such that $\Delta\mathbf{K} = (I + (\mathbf{Q} + Q)\mathbf{M}_{22}^{\mathcal{K}})^{-1}(\mathbf{Q} + Q)$.*
3. *Letting $\mathcal{K}' \in \mathbb{K}_q$ and $\Delta\mathbf{K} = \mathcal{K}' - \mathcal{K} \in \mathbb{K}$, it holds that $Q(\Delta\mathbf{K}) = \Delta\mathbf{K}$ and*

$$\mathbf{Q}(\Delta\mathbf{K})(s) = \Delta\mathbf{K} \begin{bmatrix} C & 0 \\ 0 & I \end{bmatrix} (sI - \begin{bmatrix} A & BC_{\mathcal{K}'} \\ B_{\mathcal{K}'}C & A_{\mathcal{K}'} \end{bmatrix})^{-1} \begin{bmatrix} B & 0 \\ 0 & I \end{bmatrix} \Delta\mathbf{K}.$$

Proof. The first and second conclusions can be verified by Youla parameterization [34]. Since both \mathbb{K}_q and \mathbb{K} are defined as sets of controllers that ensure internal stability of the closed-loop system, the invertibility of all the relevant matrices (such as $I - \mathbf{M}_{22}^{\mathcal{K}}\Delta\mathbf{K}$ and $I + (\mathbf{Q} + Q)\mathbf{M}_{22}^{\mathcal{K}}$) is guaranteed by construction.

For the third conclusion, note that $\Delta\mathbf{K}(I - \mathbf{M}_{22}^{\mathcal{K}}\Delta\mathbf{K})^{-1}$ has a realization:

$$\dot{\xi}_t = \begin{bmatrix} A & BC_{\mathcal{K}'} \\ B_{\mathcal{K}'}C & A_{\mathcal{K}'} \end{bmatrix} \xi_t + \begin{bmatrix} B & 0 \\ 0 & I \end{bmatrix} \Delta\mathbf{K}u_t, \quad y_t = \Delta\mathbf{K} \begin{bmatrix} C & 0 \\ 0 & I \end{bmatrix} \xi_t + \Delta\mathbf{K}u_t \quad (63)$$

with $\mathcal{K}' = \mathcal{K} + \Delta\mathbf{K}$. Based on this realization, we let

$$\mathbf{Q}(\Delta\mathbf{K})(s) = \Delta\mathbf{K} \begin{bmatrix} C & 0 \\ 0 & I \end{bmatrix} (sI - \begin{bmatrix} A & BC_{\mathcal{K}'} \\ B_{\mathcal{K}'}C & A_{\mathcal{K}'} \end{bmatrix})^{-1} \begin{bmatrix} B & 0 \\ 0 & I \end{bmatrix} \Delta\mathbf{K}, \quad Q(\Delta\mathbf{K}) = \Delta\mathbf{K}. \quad (64)$$

This completes the proof. \square

Remark 5.2. All the inverses in Lemma 5.1 are well-defined, since both \mathbb{K}_q and \mathbb{K} are defined as sets of controllers stabilizing system (8). As a result, the relevant closed-loop transfer matrices are invertible for all \mathcal{K} and $\Delta\mathbf{K}$ under consideration.

Building on the above translation, we lift the feasible set of the original controller optimization problem (8) to an infinite-dimensional parameter space \mathbb{U} associated with an arbitrary initial controller $\mathcal{K} \in \mathbb{K}_q$. Crucially, by the mapping described in Lemma 5.1, the closed-loop term $\Delta\mathbf{K}(I - \mathbf{M}_{22}^\mathcal{K}\Delta\mathbf{K})^{-1}$ in the objective can be represented as $(\mathbf{Q} + Q)$. Replacing this term in the cost functional of problem (8) yields the following equivalent performance index:

$$J_{\mathcal{K}}(\mathbf{Q}, Q) := \|\mathbf{M}_{11}^\mathcal{K} + \mathbf{M}_{12}^\mathcal{K}(\mathbf{Q} + Q)\mathbf{M}_{21}^\mathcal{K}\|_{\mathcal{H}_2}^2, \quad \forall (\mathbf{Q}, Q) \in \mathbb{U}.$$

It is this new objective function that forms the focus of our subsequent analysis. Notably, the original nonlinear term in the objective is now replaced by a linear parameterization in the convex set \mathbb{U} , rendering the problem convex. This convexity permits the application of efficient convex optimization methods and provides a foundation for the theoretical development that follows.

To facilitate the analysis, we introduce the following inner product on \mathbb{U} :

$$\langle (\mathbf{Q}, Q), (\mathbf{Q}', Q') \rangle_{\mathbb{U}} := \langle \mathbf{Q}, \mathbf{Q}' \rangle_{\mathcal{H}_2} + \langle Q, Q' \rangle_F \quad (65)$$

with the corresponding norm

$$\|(\mathbf{Q}, Q)\|_{\mathbb{U}} := \sqrt{\|\mathbf{Q}\|_{\mathcal{H}_2}^2 + \|Q\|_F^2} \quad (66)$$

We also define an operator $\mathcal{S}[\cdot]$ that extracts the stable part of any transfer function matrix. That is, for any transfer matrix $\mathbf{N}(s)$, we have a unique decomposition $\mathbf{N}(s) = \mathbf{N}_1(s) + \mathbf{N}_2(s)$ (see Sec 3 in [42] for details), where $\mathbf{N}_1(s)$ is stable and $\mathbf{N}_2(s)$ is anti-stable, and then we set $\mathcal{S}[\mathbf{N}(s)] := \mathbf{N}_1(s)$.

The enlargement from \mathbb{K}_q to \mathbb{U} fundamentally resolves the two main limitations discussed in Remark 4.2. First, by extending the parameter space to the infinite-dimensional set \mathbb{U} , all the structural restrictions on the feasible set are removed so that arbitrary search directions can be explored. Second, $J_{\mathcal{K}}$ becomes convex over \mathbb{U} , and thus any stationary point is globally optimal. In particular, as shown in the following theorem, the gradient of $J_{\mathcal{K}}(\mathbf{Q}, Q)$ contains a transfer function matrix that precisely recovers the frequency-domain optimality condition characterized previously (see Theorem 3.4). Consequently, the essential frequency-domain information is fully preserved throughout the optimization process. With notations (65) and (66), we can analyze the gradient, smoothness, and other optimization properties of $J_{\mathcal{K}}(\mathbf{Q}, Q)$ in the convex and structurally unconstrained parameter space \mathbb{U} .

Theorem 5.3. *Let $\mathcal{K} \in \mathbb{K}_q$ be a given initial controller. Then, the Fréchet derivative of the cost functional $J_{\mathcal{K}}$ with respect to $(\mathbf{Q}, Q) \in \mathbb{U}$ is given by*

$$\nabla J_{\mathcal{K}}(\mathbf{Q}, Q) = 2(\mathbf{S}, \mathbf{e}_{(q+m_1) \times (q+m_2)}(\text{Res}_{\Re(s) \leq 0}(\mathbf{S}), m_1, m_2)),$$

where

$$\mathbf{S}(s) = \mathcal{S}\left[(\mathcal{C}_1 - \mathcal{B}_1\mathcal{P}_{\mathcal{K}})(sI - \mathcal{A})^{-1}(\mathcal{B}_0 - \Sigma_{\mathcal{K}}\mathcal{C}_0) + (\mathbf{M}_{12}^\mathcal{K}(-s))^\top \mathbf{M}_{12}^\mathcal{K}(\mathbf{Q}(s) + Q)\mathbf{M}_{21}^\mathcal{K}(s)(\mathbf{M}_{21}^\mathcal{K}(-s))^\top\right].$$

Proof. Consider the perturbed cost functional with variation $(\Delta\mathbf{Q}, \Delta Q)$

$$\begin{aligned} J_{\mathcal{K}}(\mathbf{Q} + \Delta\mathbf{Q}, Q + \Delta Q) &= \|\mathbf{M}_{11}^\mathcal{K} + \mathbf{M}_{12}^\mathcal{K}(\mathbf{Q}(s) + Q + \Delta\mathbf{Q} + \Delta Q)\mathbf{M}_{21}^\mathcal{K}\|_{\mathcal{H}_2}^2 \\ &= \|\mathbf{M}_{11}^\mathcal{K} + \mathbf{M}_{12}^\mathcal{K}(\mathbf{Q} + Q)\mathbf{M}_{21}^\mathcal{K}\|_{\mathcal{H}_2}^2 \\ &\quad + 2 \int_{-\infty}^{\infty} \text{tr} \left[\left(\mathbf{M}_{11}^\mathcal{K}(j\omega) + \mathbf{M}_{12}^\mathcal{K}(j\omega)(\mathbf{Q}(j\omega) + Q)\mathbf{M}_{21}^\mathcal{K}(j\omega) \right)^* \mathbf{M}_{12}^\mathcal{K}(j\omega)\Delta\mathbf{Q}(j\omega) \right. \\ &\quad \left. \times \mathbf{M}_{21}^\mathcal{K}(j\omega) \right] \frac{d\omega}{2\pi} + 2 \text{tr}(\text{Res}_{\Re(s) \leq 0}(\mathbf{S}(s))\Delta Q^\top) + \mathcal{O}(\|(\Delta\mathbf{Q}, \Delta Q)\|_{\mathbb{U}}^2). \end{aligned}$$

The first-order term can be rewritten as

$$2 \int_{-\infty}^{\infty} \text{tr} \left(\mathbf{M}_{21}^\mathcal{K}(j\omega)^* \Delta\mathbf{Q}(j\omega)^* \mathbf{M}_{12}^\mathcal{K}(j\omega)^* (\mathbf{M}_{11}^\mathcal{K}(j\omega) + \mathbf{M}_{12}^\mathcal{K}(j\omega)(\mathbf{Q}(j\omega) + Q)\mathbf{M}_{21}^\mathcal{K}(j\omega)) \right) \frac{d\omega}{2\pi}$$

$$+ 2 \operatorname{tr}(\operatorname{Res}_{\Re(s) \leq 0}(\mathbf{S}(s))\Delta Q^\top).$$

By Lemma 3.3, this expression simplifies to

$$2 \int_{-\infty}^{\infty} \operatorname{tr} \left[\left(\mathbf{S}(j\omega)^* \Delta(\mathbf{Q}(j\omega)) \right) \right] \frac{d\omega}{2\pi} + 2 \operatorname{tr}(\operatorname{Res}_{\Re(s) \leq 0}(\mathbf{S}(s))\Delta Q^\top).$$

Noting $\Delta Q \in \mathbb{R}^{(q+m_1) \times (q+m_2) | m_1 \times m_2}$, we can get

$$\begin{aligned} & 2 \int_{-\infty}^{\infty} \operatorname{tr} \left[\left(\mathbf{S}(j\omega)^* \Delta(\mathbf{Q}(j\omega)) \right) \right] \frac{d\omega}{2\pi} + 2 \operatorname{tr}(\operatorname{Res}_{\Re(s) \leq 0}(\mathbf{S}(s))\Delta Q^\top) \\ &= 2 \int_{-\infty}^{\infty} \operatorname{tr} \left[\left(\mathbf{S}(j\omega)^* \Delta(\mathbf{Q}(j\omega)) \right) \right] \frac{d\omega}{2\pi} + 2 \operatorname{tr}(\mathbf{e}_{(q+m_1) \times (q+m_2)} (\operatorname{Res}_{\Re(s) \leq 0}(\mathbf{S}(s)), m_1, m_2) \Delta Q^\top). \end{aligned}$$

The result follows from the definition of the stable projection $\mathcal{S}[\cdot]$. \square

Lemma 5.4. (*Lipschitz smoothness of $J_{\mathcal{K}}$*) Let \mathcal{K} be any stabilizing controller of system (8). Then, the cost functional $J_{\mathcal{K}}(\mathbf{Q}, Q)$ is Lipschitz smooth with respect to (\mathbf{Q}, Q) . Specifically, there exists a constant $L_{\mathcal{K}} > 0$, which depends only on the controller \mathcal{K} , such that for any pair $(\mathbf{Q}, Q), (\mathbf{Q}', Q') \in \mathbb{U}$, the following inequality holds:

$$\begin{aligned} J_{\mathcal{K}}(\mathbf{Q}, Q) &\leq J_{\mathcal{K}}(\mathbf{Q}', Q') + \langle \nabla J_{\mathcal{K}}(\mathbf{Q}', Q'), (\mathbf{Q} - \mathbf{Q}', Q - Q') \rangle_{\mathbb{U}} \\ &\quad + \frac{L_{\mathcal{K}}}{2} (\|\mathbf{Q} - \mathbf{Q}'\|_{\mathcal{H}_2}^2 + \|Q - Q'\|_F^2), \end{aligned} \tag{67}$$

where $\nabla J_{\mathcal{K}}(\mathbf{Q}', Q')$ denotes the gradient evaluated at (\mathbf{Q}', Q') .

Proof. To streamline the notation, let us define the perturbations as $\Delta \mathbf{Q} = \mathbf{Q} - \mathbf{Q}'$ and $\Delta Q = Q - Q'$. First, we expand $J_{\mathcal{K}}(\mathbf{Q}, Q)$ around $J_{\mathcal{K}}(\mathbf{Q}', Q')$. Using the definition from (24), we get

$$J_{\mathcal{K}}(\mathbf{Q}, Q) = J_{\mathcal{K}}(\mathbf{Q}', Q') + \langle \nabla J_{\mathcal{K}}(\mathbf{Q}', Q'), (\Delta \mathbf{Q}, \Delta Q) \rangle_{\mathbb{U}} + \|\mathbf{M}_{12}^{\mathcal{K}}(\Delta \mathbf{Q} + \Delta Q)\mathbf{M}_{21}^{\mathcal{K}}\|_{\mathcal{H}_2}^2.$$

Here, the linear terms correspond precisely to the inner product with the gradient at (\mathbf{Q}', Q') .

The next step is to bound the quadratic term $\|\mathbf{M}_{12}^{\mathcal{K}}(\Delta \mathbf{Q} + \Delta Q)\mathbf{M}_{21}^{\mathcal{K}}\|_{\mathcal{H}_2}^2$. Using the inequality $\|A + B\|^2 \leq 2\|A\|^2 + 2\|B\|^2$, $\|\mathbf{M}_{12}^{\mathcal{K}}(\Delta \mathbf{Q} + \Delta Q)\mathbf{M}_{21}^{\mathcal{K}}\|_{\mathcal{H}_2}^2$ can be expressed as

$$\|\mathbf{M}_{12}^{\mathcal{K}}(\Delta \mathbf{Q} + \Delta Q)\mathbf{M}_{21}^{\mathcal{K}}\|_{\mathcal{H}_2}^2 \leq 2\|\mathbf{M}_{12}^{\mathcal{K}}\Delta \mathbf{Q}\mathbf{M}_{21}^{\mathcal{K}}\|_{\mathcal{H}_2}^2 + 2\|\mathbf{M}_{12}^{\mathcal{K}}\Delta Q\mathbf{M}_{21}^{\mathcal{K}}\|_{\mathcal{H}_2}^2. \tag{68}$$

We now bound each of these two terms using properties of \mathcal{H}_{∞} and \mathcal{H}_2 norms, as well as the residue theorem for the constant term. This leads to the following detailed bound:

$$\begin{aligned} & \|\mathbf{M}_{12}^{\mathcal{K}}(\Delta \mathbf{Q} + \Delta Q)\mathbf{M}_{21}^{\mathcal{K}}\|_{\mathcal{H}_2}^2 \\ & \leq 2 \left(\frac{\|\mathbf{M}_{12}^{\mathcal{K}}\|_{\mathcal{H}_{\infty}}^2 \|\mathbf{M}_{21}^{\mathcal{K}}\|_{\mathcal{H}_{\infty}}^2}{2\pi} \int_{-\infty}^{\infty} \operatorname{tr}(\Delta \mathbf{Q}(j\omega)^* \Delta \mathbf{Q}(j\omega)) d\omega \right) \\ & \quad + 2 \operatorname{tr}(\operatorname{Res}_{\Re(s) \leq 0}((\mathbf{M}_{21}^{\mathcal{K}}(-s))^{\top} \mathbf{M}_{21}^{\mathcal{K}}(s) \Delta Q (\mathbf{M}_{12}^{\mathcal{K}}(-s))^{\top} \mathbf{M}_{12}^{\mathcal{K}}(s) \Delta Q^{\top})). \end{aligned}$$

Recognizing $\|\Delta \mathbf{Q}\|_{\mathcal{H}_2}^2 = \frac{1}{2\pi} \int_{-\infty}^{\infty} \operatorname{tr}(\Delta \mathbf{Q}(j\omega)^* \Delta \mathbf{Q}(j\omega)) d\omega$ and that the residue term is bounded by $C'_{\mathcal{K}} \|\Delta Q\|_F^2$ for some constant $C'_{\mathcal{K}}$ (from Lemma 3.3), we can see that there must exist a constant $L_{\mathcal{K}} > 0$ such that

$$\|\mathbf{M}_{12}^{\mathcal{K}}(\Delta \mathbf{Q} + \Delta Q)\mathbf{M}_{21}^{\mathcal{K}}\|_{\mathcal{H}_2}^2 \leq \frac{L_{\mathcal{K}}}{2} (\|\Delta \mathbf{Q}\|_{\mathcal{H}_2}^2 + \|\Delta Q\|_F^2).$$

Substituting this bound back into our expansion for $J_{\mathcal{K}}(\mathbf{Q}, Q)$ yields the inequality (67). This establishes that $J_{\mathcal{K}}$ is Lipschitz smooth, and an explicit value for the constant $L_{\mathcal{K}}$ can be constructed from the bounds derived above. This completes the proof. \square

5.2 The Gradient-Based Method and Convergence Analysis

In this section, we present the gradient-based method and analyze its convergence rate.

Algorithm 1: Iterative Update of $\mathbf{Q}_k(s)$

Input: Initial controller \mathcal{K}_0 ; system matrices $(\mathcal{A}_0, \mathcal{B}_0^0, \mathcal{B}_1, \mathcal{C}_0, \mathcal{C}_1^0)$; step size η ; maximum iteration N ;

Output: Sequences $\{\mathbf{Q}_k(s)\}$, $\{Q_k\}$, $\{\Delta\mathbf{K}_{k+1}\}$, the final controller \mathcal{K}_N ;

Initialize $\mathbf{Q}_0(s) \leftarrow 0_{(q+m_1) \times (q+m_2)}$;

Initialize $Q_0 \leftarrow 0_{(q+m_1) \times (q+m_2)}$;

for $k = 0$ **to** $N - 1$ **do**

Compute:

$$\mathbf{S}_k(s) \leftarrow \mathcal{S} \left[(\mathcal{C}_1^0 - \mathcal{B}_1 \mathcal{P}_{\mathcal{K}_0})(sI - \mathcal{A}_0)^{-1} (\mathcal{B}_0^0 - \Sigma_{\mathcal{K}_0} \mathcal{C}_0) \right. \\ \left. + (\mathbf{M}_{12}^{\mathcal{K}_0}(-s))^\top \mathbf{M}_{12}^{\mathcal{K}_0}(s) (\mathbf{Q}_k(s) + Q_k) \mathbf{M}_{21}^{\mathcal{K}_0}(s) (\mathbf{M}_{21}^{\mathcal{K}_0}(-s))^\top \right]$$

// Obtain the stable part via modal decomposition and removing unstable modes.

Update $\mathbf{Q}_{k+1}(s) \leftarrow \mathbf{Q}_k(s) - \eta \mathbf{S}_k(s)$;

Update $Q_{k+1} \leftarrow Q_k - \eta \mathbf{e}_{(q+m_1) \times (q+m_2)}(\text{Res}_{\Re(s) \leq 0}(\mathbf{S}_k(s)), m_1, m_2)$;

Update $\Delta\mathbf{K}_{k+1} \leftarrow (I + (\mathbf{Q}_{k+1}(s) + Q_{k+1}) \mathbf{M}_{22}^{\mathcal{K}_0})^{-1} (\mathbf{Q}_{k+1}(s) + Q_{k+1})$;

$\mathcal{K}_N \leftarrow \mathcal{F}(\mathcal{K}_0, \Delta\mathbf{K}_N)$;

return $\{\mathbf{Q}_k(s)\}$, $\{Q_k\}$, $\{\Delta\mathbf{K}_{k+1}\}$, \mathcal{K}_N ;

Remark: All the inverses in Algorithm 1 are well-defined in every iteration according to Youla parametrization.

In the Algorithm 1 above,

$$\mathcal{A}_0 = \begin{bmatrix} A & BC_{\mathcal{K}_0} \\ B_{\mathcal{K}_0} C & A_{\mathcal{K}_0} \end{bmatrix}, \quad \mathcal{B}_0^0 = \begin{bmatrix} 0 & 0 \\ B_{\mathcal{K}_0} \mathcal{V} & 0 \end{bmatrix}, \quad \mathcal{C}_1^0 = \begin{bmatrix} 0 & RC_{\mathcal{K}_0} \\ 0 & 0 \end{bmatrix}.$$

and the operator \mathcal{F} is defined as follows. At the final iteration, let $G_{\mathcal{K}_0}$ denote the nominal closed-loop system (the generalized plant formed by interconnecting the original plant with the initial controller parameter \mathcal{K}_0). The update $\Delta\mathbf{K}_N$, designed to improve the performance, is then interconnected with $G_{\mathcal{K}_0}$ via a lower Linear Fractional Transformation (LFT), as illustrated in [42, Section 10.1]. The final controller \mathcal{K}_N is then defined as the overall input-output map of the interconnected system, which can be expressed by

$$\mathcal{K}_N = \mathcal{F}(\mathcal{K}_0, \Delta\mathbf{K}_N) := \text{minreal}(\mathcal{L}(G_{\mathcal{K}_0}, \Delta\mathbf{K}_N));$$

here, $\mathcal{L}(G_{\mathcal{K}_0}, \Delta\mathbf{K}_N)$ denotes the lower LFT interconnection of $G_{\mathcal{K}_0}$ and $\Delta\mathbf{K}_N$. The $\text{minreal}(\cdot)$ operation extracts the minimal state-space realization to yield the final controller in the standard form:

$$\mathcal{K}_N = \begin{bmatrix} 0 & C_{\mathcal{K}_N} \\ B_{\mathcal{K}_N} & A_{\mathcal{K}_N} \end{bmatrix}.$$

Theorem 5.5 (Lipschitz Continuity of the Gradient). *The gradient of $J_{\mathcal{K}_0}$ is L -Lipschitz continuous on \mathbb{U} ; that is, there exists a constant $L > 0$ such that for any $(\mathbf{Q}, Q), (\mathbf{Q}', Q') \in \mathbb{U}$,*

$$\frac{1}{L} \|\nabla J_{\mathcal{K}_0}(\mathbf{Q}', Q') - \nabla J_{\mathcal{K}_0}(\mathbf{Q}, Q)\|_{\mathbb{U}}^2 \leq \langle \nabla J_{\mathcal{K}_0}(\mathbf{Q}', Q') - \nabla J_{\mathcal{K}_0}(\mathbf{Q}, Q), \Delta \rangle_{\mathbb{U}} \quad (69)$$

holds with $\Delta = (\mathbf{Q}', Q') - (\mathbf{Q}, Q)$.

Proof. Consider the auxiliary function

$$\phi(\hat{\mathbf{Q}}, \hat{Q}) := J_{\mathcal{K}_0}(\hat{\mathbf{Q}}, \hat{Q}) - \langle \nabla J_{\mathcal{K}_0}(\mathbf{Q}, Q), (\hat{\mathbf{Q}}, \hat{Q}) \rangle_{\mathbb{U}}, \forall (\hat{\mathbf{Q}}, \hat{Q}) \in \mathbb{U},$$

which is convex and achieves its minimum at (\mathbf{Q}, Q) . Since $J_{\mathcal{K}_0}$ is $L_{\mathcal{K}_0}$ -smooth, the function ϕ is also $L_{\mathcal{K}_0}$ -smooth. A direct consequence of the $L_{\mathcal{K}_0}$ -smoothness of ϕ is the following inequality:

$$\phi(\mathbf{Q}, Q) \leq \phi(\mathbf{Q}', Q') + \langle \nabla \phi(\mathbf{Q}', Q'), (\hat{\mathbf{Q}}, \hat{Q}) - (\mathbf{Q}', Q') \rangle_{\mathbb{U}} + \frac{L_{\mathcal{K}_0}}{2} \|(\hat{\mathbf{Q}}, \hat{Q}) - (\mathbf{Q}', Q')\|_{\mathbb{U}}^2.$$

Taking $(\hat{\mathbf{Q}}, \hat{Q}) - (\mathbf{Q}', Q') = \nabla \phi(\mathbf{Q}', Q')$ into (70), we have

$$\phi(\mathbf{Q}, Q) \leq \phi(\mathbf{Q}', Q') - \frac{1}{2L_{\mathcal{K}_0}} \|\nabla \phi(\mathbf{Q}', Q')\|_{\mathbb{U}}^2. \quad (70)$$

By swapping the roles of (\mathbf{Q}, Q) and (\mathbf{Q}', Q') in the derivation, we obtain another inequality:

$$\phi(\mathbf{Q}', Q') \leq \phi(\mathbf{Q}, Q) - \frac{1}{2L_{\mathcal{K}_0}} \|\nabla \phi(\mathbf{Q}', Q')\|_{\mathbb{U}}^2. \quad (71)$$

Setting $L = L_{\mathcal{K}_0}$ and combining (70) with (71) leads to the desired result (69). \square

Remark 5.6. This result constitutes a nontrivial extension of the classic Lipschitz continuity (or smoothness) of the gradient of the cost functional in finite-dimensional Euclidean space (see, e.g., [20, Sec. 2.1]), to the infinite-dimensional setting, with two notable distinctions:

- The gradient operator $\nabla J_{\mathcal{K}_0}(\mathbf{Q}, Q)$ is defined with respect to transfer functions (see Theorem 5.3), in contrast to gradients in Euclidean spaces, which are defined with respect to finite-dimensional vectors.
- The inner product $\langle \cdot, \cdot \rangle_{\mathbb{U}}$ is, by construction, a composite of the \mathcal{H}_2 inner product and the standard Euclidean inner product, taking into account both the transfer function and the static gain components.

Building on Theorem 5.5, we now establish the convergence of Algorithm 1.

Theorem 5.7 (Sublinear Convergence). *Provided that the step size satisfies $\eta < 2/L_{\mathcal{K}_0}$, the sequence of objective functional, $\{J_{\mathcal{K}_0}(\mathbf{Q}_k, Q_k)\}_{k \geq 0}$, generated by Algorithm 1 converges sublinearly to the optimal value of LQG problem.*

Proof. Let \mathcal{K}^* denote an optimal controller, and let

$$r_k = \sqrt{\|\mathbf{Q}_k - \mathbf{Q}_{\mathcal{K}^*}\|_{\mathcal{H}_2}^2 + \|Q_k - Q_{\mathcal{K}^*}\|_F^2},$$

where $(\mathbf{Q}_{\mathcal{K}^*}, Q_{\mathcal{K}^*})$ is the optimal solution associated with $\mathcal{K}^* \in \mathbb{K}_q$. For the update step,

$$\begin{aligned} r_{k+1}^2 &= \|(\mathbf{Q}_k, Q_k) - (\mathbf{Q}_{\mathcal{K}^*}, Q_{\mathcal{K}^*}) - \eta \nabla J_{\mathcal{K}_0}(\mathbf{Q}_k, Q_k)\|_{\mathbb{U}}^2 \\ &= \|(\mathbf{Q}_k, Q_k) - (\mathbf{Q}_{\mathcal{K}^*}, Q_{\mathcal{K}^*})\|_{\mathbb{U}}^2 - 2\eta \langle \nabla J_{\mathcal{K}_0}(\mathbf{Q}_k, Q_k), (\mathbf{Q}_k, Q_k) - (\mathbf{Q}_{\mathcal{K}^*}, Q_{\mathcal{K}^*}) \rangle_{\mathbb{U}} \\ &\quad + \eta^2 \|\nabla J_{\mathcal{K}_0}(\mathbf{Q}_k, Q_k)\|_{\mathbb{U}}^2 \\ &\leq r_k^2 - 2\eta \left(\frac{1}{L_{\mathcal{K}_0}} \|\nabla J_{\mathcal{K}_0}(\mathbf{Q}_k, Q_k)\|_{\mathbb{U}}^2 \right) + \eta^2 \|\nabla J_{\mathcal{K}_0}(\mathbf{Q}_k, Q_k)\|_{\mathbb{U}}^2 \quad (\text{by Theorem 5.5}) \\ &= r_k^2 - \eta \left(\frac{2}{L_{\mathcal{K}_0}} - \eta \right) \|\nabla J_{\mathcal{K}_0}(\mathbf{Q}_k, Q_k)\|_{\mathbb{U}}^2. \end{aligned}$$

Since $\eta < 2/L_{\mathcal{K}_0}$, the coefficient of $\|\nabla J_{\mathcal{K}_0}(\mathbf{Q}_k, Q_k)\|_{\mathbb{U}}^2$ in the last equality, i.e., $\eta \left(\frac{2}{L_{\mathcal{K}_0}} - \eta \right)$, is positive, which guarantees the monotonic decrease of r_k^2 .

Due to the convexity of $J_{\mathcal{K}_0}(\cdot)$, it holds that

$$J_{\mathcal{K}_0}(\mathbf{Q}_k, Q_k) - J_{\mathcal{K}_0}(\mathbf{Q}_{\mathcal{K}^*}, Q_{\mathcal{K}^*}) \leq \langle \nabla J_{\mathcal{K}_0}(\mathbf{Q}_k, Q_k), \Delta_k \rangle \leq r_0 \|\nabla J_{\mathcal{K}_0}(\mathbf{Q}_k, Q_k)\|_{\mathbb{U}}.$$

By the (descent) lemma for L -smooth convex functions, one has

$$J_{\mathcal{K}_0}(\mathbf{Q}_{k+1}, Q_{k+1}) \leq J_{\mathcal{K}_0}(\mathbf{Q}_k, Q_k) - \eta \left(1 - \frac{L_{\mathcal{K}_0}}{2} \eta \right) \|\nabla J_{\mathcal{K}_0}(\mathbf{Q}_k, Q_k)\|_{\mathbb{U}}^2.$$

Thus,

$$\Delta J_{\mathcal{K}^0}(\mathbf{Q}_{k+1}, Q_{k+1}) \leq \Delta J_{\mathcal{K}^0}(\mathbf{Q}_k, Q_k) - \frac{\eta \left(1 - \frac{L_{\mathcal{K}^0} \eta}{2}\right)}{r_0^2} (\Delta J_{\mathcal{K}^0}(\mathbf{Q}_k, Q_k))^2, \quad (72)$$

where $\Delta J_{\mathcal{K}^0}(\mathbf{Q}_k, Q_k) := J_{\mathcal{K}^0}(\mathbf{Q}_k, Q_k) - J_{\mathcal{K}^0}(\mathbf{Q}_{\mathcal{K}^*}, Q_{\mathcal{K}^*})$. Inequality (72) yields the claimed sublinear convergence. \square

Remark 5.8. The preceding theoretical analysis guarantees the sublinear convergence of Algorithm 1, assuming exact computation at each iterative step. However, a practical challenge arises from the iterative growth in the order of transfer function \mathbf{Q}_k . This growth occurs because the update rule in Algorithm 1 is an additive process summing \mathbf{Q}_k with another transfer function which can increase the model's complexity with each iteration. This escalating computational cost can impede simulations with a large number of iterations and potentially introduce numerical inaccuracies. Addressing this scalability is a valuable direction for future work. One promising approach is to develop a hybrid algorithm that synergizes our method with the standard policy gradient or its variants. Such a method could leverage the computational efficiency of policy gradient for initial exploration, then switch to our algorithm to ensure convergence to the global optimum by escaping local optima and saddle points in problem (8). Another avenue involves a deeper investigation into the optimization landscape of LQG problem itself to find more structurally efficient solutions.

Remark 5.9 (Extension to the Data-Driven Setting). The analysis in this section operated under the assumption that all the system parameters are known. We further show that Algorithm 1 is extensible to a data-driven setting. This is possible because the algorithm's iterative steps do not require an explicit model of the system dynamics. Instead, the updates rely exclusively on a few key quantities—the transfer functions $\mathbf{M}_{22}^{\mathcal{K}^0}$ and $\mathbf{S}_k(s)$, and the residue $\mathbf{e}_{(q+m_1) \times (q+m_2)}(\text{Res}_{\Re(s) \leq 0}(\mathbf{S}_k(s)), m_1, m_2)$ which can be estimated directly from input-output data. We provide the detailed procedures for this estimation in Appendix A and experimentally validate their effectiveness in subsection 6.2.

6 Numerical Experiments

6.1 Example 1: Escaping a Suboptimal Stationary Point

The scalability issues associated with long-term iterations, as previously discussed, make it impractical to evaluate the Algorithm 1 over very large numbers of iterations in our experimental setting. Therefore, we focus on assessing the algorithm's performance within a small number of iterations, which is also of practical interest in many real-world scenarios where rapid convergence is desired.

In this context, we aim to demonstrate two advantageous features of Algorithm 1: its rapid initial convergence and robust ability to bypass suboptimal solutions corresponding to stationary points of problem (8). To this end, we consider the typical example from [5], a case where the vanilla policy gradient method has been shown to be trapped at a suboptimal stationary point of problem (8). This example illustrates our algorithm's performance on a complex optimization landscape. The system matrices are given by:

$$A = \begin{bmatrix} -0.5 & 0 \\ 0.5 & -1 \end{bmatrix}, \quad B = \begin{bmatrix} -1 \\ 1 \end{bmatrix}, \quad C = \begin{bmatrix} -\frac{1}{6} & \frac{11}{12} \end{bmatrix}, \quad (73)$$

and the performance weights are set as:

$$W = Q = \begin{bmatrix} 1 & 0 \\ 0 & 1 \end{bmatrix}, \quad V = R = 1.$$

The globally optimal LQG controller obtained by solving equation (6) is

$$A_{\mathcal{K}^*} = \begin{bmatrix} -1.1 & 0.13 \\ 1.19 & -1.64 \end{bmatrix}, \quad B_{\mathcal{K}^*} = \begin{bmatrix} 0.11 \\ 0.45 \end{bmatrix}, \quad C_{\mathcal{K}^*} = \begin{bmatrix} 0.62 & 0.22 \end{bmatrix}.$$

System (73) is open-loop stable, and Theorem 4.2 in [30] guarantees that all the controllers \mathcal{K} satisfying $B_{\mathcal{K}} = 0_{2 \times 1}$ and $C_{\mathcal{K}} = 0_{1 \times 2}$ are stationary points of problem (8).

We compare our proposed Algorithm 1 with the vanilla policy gradient method. For Algorithm 1, we use a step size of $\eta = 0.1$ and set the number of iterations to $N = 14$. For the vanilla policy gradient method, a larger fixed step size of $\eta_2 = 10$ and the same iteration count N are used. To evaluate and compare the performance of both methods, we adopt the normalized relative cost error as the metric. For Algorithm 1, the error at iteration k is defined as

$$\text{Error}_{\text{Q-update}} = \frac{J_{\mathcal{K}_0}(\mathbf{Q}_k, Q_k) - J(\mathcal{K}^*)}{J(\mathcal{K}^*)},$$

where $J_{\mathcal{K}_0}(\mathbf{Q}_k, Q_k)$ is the cost at iteration k and $J(\mathcal{K}^*)$ is the known optimal cost. For the vanilla policy gradient method, the error is calculated analogously as

$$\text{Error}_{\text{PG}} = \frac{J(\mathcal{K}_k) - J(\mathcal{K}^*)}{J(\mathcal{K}^*)},$$

where $J(\mathcal{K}_k)$ denotes the cost at iteration k for the policy gradient method. We conduct two experiments with initial conditions of increasing difficulty to systematically evaluate the ability of both algorithms to handle more challenging scenarios.

First, we initialize the controller at a point near the suboptimal stationary point ($B_{\mathcal{K}} = 0_{2 \times 1}$, $A_{\mathcal{K}} = -0.5I_2$, $C_{\mathcal{K}} = 0_{1 \times 2}$), as defined by:

$$A_{\mathcal{K}_0} = \begin{bmatrix} -0.5 & 0 \\ 0 & -0.5 \end{bmatrix}, \quad B_{\mathcal{K}_0} = \begin{bmatrix} 0 \\ 0.01 \end{bmatrix}, \quad C_{\mathcal{K}_0} = [0 \quad -0.01].$$

The convergence results are presented in Figure 1(a). As shown, within a small number of iterations, the vanilla policy gradient method exhibits virtually no change and fails to make any visible progress, further confirming its inability to leave the basin of attraction of this suboptimal point in the early phase of optimization. In contrast, Algorithm 1 consistently reduces the cost error, demonstrating its ability to successfully navigate away from this suboptimal region.

To create a more definitive test, we then initialize the controller exactly at the suboptimal stationary point

$$A_{\mathcal{K}_0} = \begin{bmatrix} -0.5 & 0 \\ 0 & -0.5 \end{bmatrix}, \quad B_{\mathcal{K}_0} = \begin{bmatrix} 0 \\ 0 \end{bmatrix}, \quad C_{\mathcal{K}_0} = [0 \quad 0],$$

a location where the gradient $\nabla J(\mathcal{K}_0)$ is identically zero. The outcome is shown in Figure 1(b): as expected, the vanilla policy gradient method makes no progress. Notably, even under this extreme condition where first-order information vanishes, our algorithm identifies an efficient search direction and achieves cost reduction within just 14 iterations. Interestingly, we observe that the convergence curves in this case are nearly identical to those obtained when the initial point is set near (but not exactly at) the stationary point (Figure 1(a)). The difference in performance between the two cases is tiny, with the convergence curves being nearly identical. This remarkable consistency suggests that the algorithm's performance is robust to the initial conditions within this stationary region.

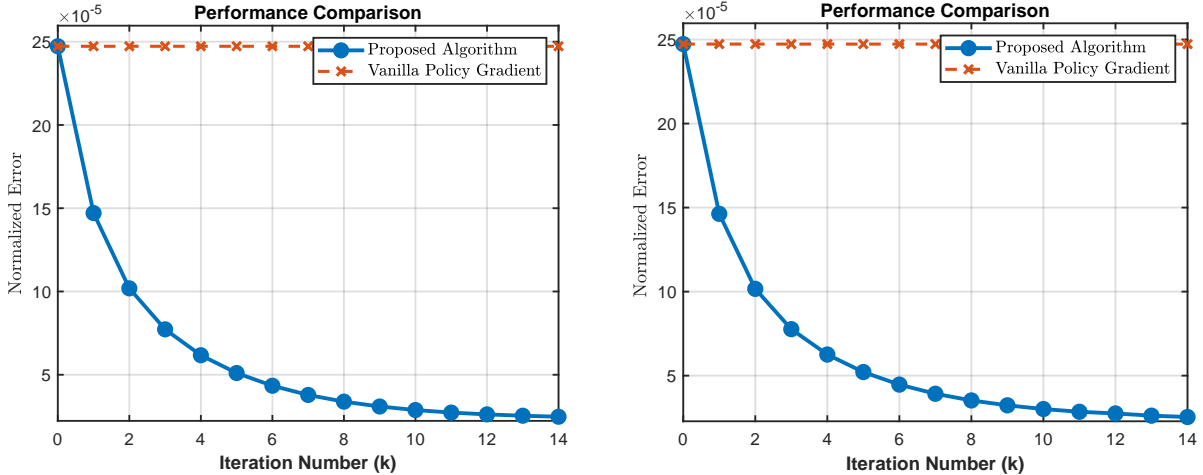
Taken together, these experiments clearly show the advantages of our method. These experiments empirically validate that our method can generate effective search directions, even at locations where first-order gradient information is unavailable. This distinguishing feature sets our algorithm apart from the vanilla policy gradient method and provides evidence of its superior convergence behavior in complex, non-convex optimization landscapes.

6.2 Example 2: Validation of Data-Driven Estimation Methods

This section validates the data-driven estimation methods proposed in Appendix A, which constitute essential components of our algorithm. Specifically, we evaluate the accuracy of estimating: 1) the transfer function matrix $\mathbf{M}_{22}^{\mathcal{K}_0}(s)$, 2) the sensitivity function $\mathbf{S}_k(s)$, and 3) the residue term $\mathbf{e}_{(q+m_1) \times (q+m_2)}(\text{Res}_{\Re(s) \leq 0}(\mathbf{S}_k(s)), m_1, m_2)$ via zeroth-order methods.

6.2.1 Experimental Setup

All the subsequent tests are conducted at the first iteration ($k = 0$) of Algorithm 1, with the system parameters fixed as specified in Example 1. Only the controller \mathcal{K}_0 is initialized with the following



(a) Case 1: Initialized near the stationary point.

(b) Case 2: Initialized exactly at the stationary point.

Figure 1: Convergence comparison between vanilla policy gradient and Algorithm 1 when initialized (a) near and (b) exactly at a sub-optimal stationary point.

state-space parameters, which serve as the basis for all the subsequent calculations:

$$A_{\mathcal{K}_0} = \begin{bmatrix} -0.5 & 0 \\ 0 & -0.5 \end{bmatrix}, \quad B_{\mathcal{K}_0} = \begin{bmatrix} 0 \\ 1 \end{bmatrix}, \quad C_{\mathcal{K}_0} = [0 \quad -1].$$

Our objective is to verify that these data-driven techniques can accurately estimate the relevant parameters based on this fixed initial controller, while keeping the system parameters unchanged.

6.2.2 Validation of $\mathbf{M}_{22}^{\mathcal{K}_0}(s)$ Estimation

First, we validate the system identification procedure for $\mathbf{M}_{22}^{\mathcal{K}_0}(s)$, as detailed in Section A.0.1. The real transfer function matrix is given by:

$$\mathbf{M}_{22}^{\mathcal{K}_0}(s) = \begin{bmatrix} \text{TF}_{11}(s) & 0 & \text{TF}_{13}(s) \\ 0 & \text{TF}_{22}(s) & 0 \\ \text{TF}_{31}(s) & 0 & \text{TF}_{33}(s) \end{bmatrix} = \begin{bmatrix} \frac{1.083s^2+0.7083s+0.08333}{s^3+2s^2+2.333s+0.4167} & 0 & \frac{-1.083s-0.1667}{s^3+2s^2+2.333s+0.4167} \\ 0 & \frac{1}{s+0.5} & 0 \\ \frac{1.083s+0.1667}{s^3+2s^2+2.333s+0.4167} & 0 & \frac{s^2+1.5s+0.5}{s^3+2s^2+2.333s+0.4167} \end{bmatrix}, \quad (74)$$

where the non-zero transfer functions $\text{TF}_{ij}(s)$, $i, j \in \{1, 2, 3\}$ are as listed in (74). We observe several zero entries in this matrix. These entries represent the decoupled input-output channels where specific inputs have no dynamic influence on certain outputs. Consequently, these channels exhibit a null frequency response, making them irrelevant for our data-driven fitting process. We therefore focus on identifying only the non-zero elements. To generate the dataset for this validation, we simulate the ideal, noise-free scenario discussed in Section A.0.1. Specifically, we compute the exact frequency response of each non-zero element of the true transfer function matrix $\mathbf{M}_{22}^{\mathcal{K}_0}(s)$ from (74) at the 200 frequency points specified below. This resulting set of complex values serves as the empirical data for the fitting algorithm. This approach allows us to isolate and verify the intrinsic accuracy of the parameter fitting procedure itself, separate from the effects of stochastic noise.

The estimation is performed under the following settings:

- **Model Order:** Numerator degree $n_{deg,1} = 2$, denominator degree $n_{deg,2} = 3$.
- **Frequency Sampling:** 200 frequency points sampled at uniform intervals from 0.1 to 100 rad/s.
- **Frequency Weighting:** Uniform weight $c_\omega = 1$.

The resulting errors between the real and estimated parameters are presented in Table 1, which demonstrates a high degree of accuracy and validates the effectiveness of the fitting procedure.

Table 1: Relative error between real and estimated coefficients for non-zero elements of $\mathbf{M}_{22}^{\mathcal{K}_0}(s)$.

Error Type ($\ \text{Real Coeff} - \text{estimated Coeff}\ _\infty$)	TF ₁₁ (s)	TF ₁₃ (s)	TF ₂₂ (s)	TF ₃₁ (s)	TF ₃₃ (s)
Numerator Coeff. Error (%)	0.0067	0.0016	0	0.0013	0.0002
Denominator Coeff. Error (%)	0.0067	0.0014	0	0.0018	0

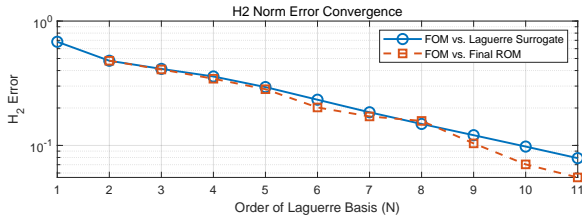
6.2.3 Validation of $\mathbf{S}_0(s)$ Estimation

Next, we evaluate the projection-based estimation of the sensitivity function $\mathbf{S}_0(s)$ (from Section A.0.2). The fitted order model (FOM) is

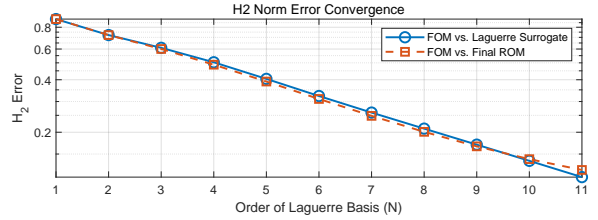
$$\mathbf{S}_0(s) = \begin{bmatrix} \mathbf{S}_0(s)_{11} & 0 & \mathbf{S}_0(s)_{13} \\ 0 & 0 & 0 \\ \mathbf{S}_0(s)_{31} & 0 & \mathbf{S}_0(s)_{33} \end{bmatrix} = \begin{bmatrix} \frac{-0.8676s^2 - 2.908s - 1.671}{s^3 + 2s^2 + 2.333s + 0.4167} & 0 & \frac{-1.513s^2 - 2.916s - 2.081}{s^3 + 2s^2 + 2.333s + 0.4167} \\ 0 & 0 & 0 \\ \frac{1.513s^2 + 2.916s + 2.081}{s^3 + 2s^2 + 2.333s + 0.4167} & 0 & \frac{1.774s^2 + 2.921s + 2.683}{s^3 + 2s^2 + 2.333s + 0.4167} \end{bmatrix}.$$

Similarly, we focus on identifying the non-zero elements. For the purpose of this validation, we leverage the known analytical form of the true sensitivity function $\mathbf{S}_0(s)$ to generate the real data. Instead of estimating the Laguerre coefficients via directional derivatives of the performance index as described in Section A.0.2, we compute them directly and with high precision by calculating the \mathcal{H}_2 inner product (i.e., projection) of the true $\mathbf{S}_0(s)$ onto each Laguerre basis function. This yields an ideal, error-free set of coefficients for constructing the Laguerre basis approximation, $\hat{\mathbf{S}}_0(s)$. The subsequent reduced-order fitting is then performed on the frequency response of this Laguerre approximation. This approach allows us to decouple the validation of the approximation and reduction steps from the numerical errors inherent in the derivative-based estimation process.

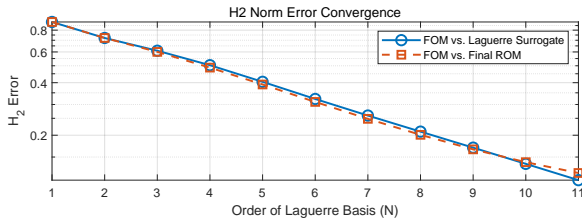
The system is first approximated using a Laguerre basis expansion with order varying from 1 to 11. Next, we fit a reduced-order transfer function model (numerator degree $n_{deg,1} = 2$ and denominator degree $n_{deg,2} = 3$) to the Laguerre-based approximation. Figure 2 illustrates the \mathcal{H}_2 norm of the estimation error for all the non-zero elements of $\mathbf{S}_0(s)$, showing both the error from the Laguerre expansion (as a function of order) and from the reduced-order model. The plots show that as the Laguerre basis order increases, the estimation error decreases rapidly for both the approaches. This confirms that the Laguerre basis efficiently represents system dynamics, and the reduced-order model accurately captures behavior when the Laguerre approximation is sufficiently accurate. In practice, a Laguerre basis of order around 10 to 15 suffices for a highly accurate reduced-order model.



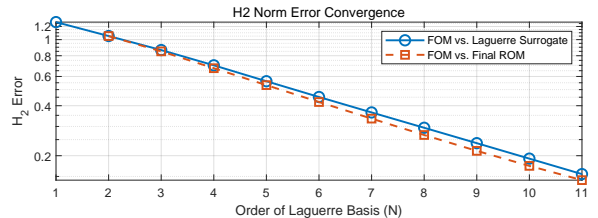
(a) Estimation error for $\mathbf{S}_0(s)_{11}$.



(b) Estimation error for $\mathbf{S}_0(s)_{13}$.



(c) Estimation error for $\mathbf{S}_0(s)_{31}$.



(d) Estimation error for $\mathbf{S}_0(s)_{33}$.

Figure 2: Convergence of the \mathcal{H}_2 estimation error for the non-zero elements of the sensitivity matrix $\mathbf{S}_0(s)$: comparison between Laguerre basis expansion and reduced-order model (both as functions of Laguerre basis order).

6.2.4 Validation of Residue Estimation

Finally, we test the Monte Carlo based estimation of the residue term $\mathbf{e}_{3 \times 3}(\text{Res}_{\mathcal{R}(s) \leq 0}(\mathbf{S}_0(s)), 1, 1)$ (from Section A.0.3). The key parameters for this simulation are set as:

- **Radius of Sampling Sphere (r):** 1×10^{-5} .
- **Sample Number:** $m = 10, 100, 1000, 10000$.

Figure 3 and Table 2 collectively demonstrate the method’s performance. The heatmaps in Figure 3 provide a qualitative visualization, showing the estimated gradient converging toward the true sparse structure as the number of Monte Carlo samples (m) increases. The quantitative results in Table 2 confirm this trend, with the relative error asymptotically decreasing from a highly inaccurate 110.8% at $m = 10$ to a precise 1.99% at $m = 10,000$.

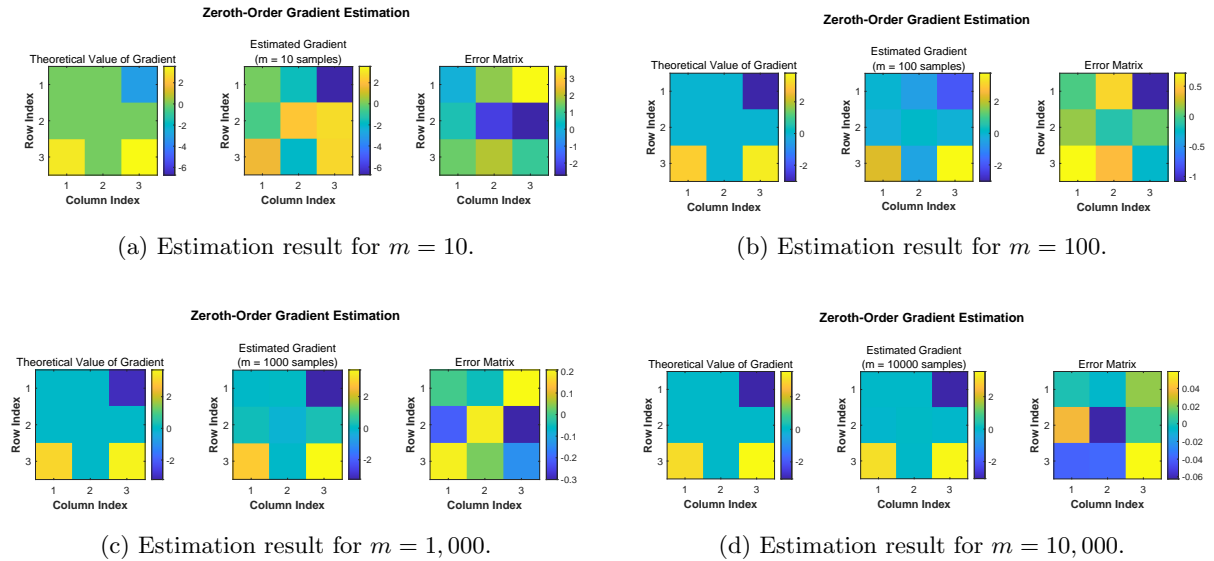


Figure 3: Qualitative convergence of the zeroth-order gradient estimate as the number of Monte Carlo samples (m) increases.

Table 2: Quantitative relative error of the zeroth-order gradient estimation under different sample sizes.

Sample Size (m)	10	100	1,000	10,000
Relative Error ($\ \text{Error Matrix}\ _F / \ \text{Real Value}\ _F$) (%)	110.82	18.84	7.03	1.99

7 Conclusion

This paper investigates the direct policy optimization of Linear Quadratic Gaussian (LQG) control. We proposed a verifiable necessary and sufficient condition for global optimality, which serves as a computationally tractable certificate and offers insights into the emergence of suboptimal stationary points in traditional parameterizations. Based on this condition, we developed a gradient-based algorithm in the infinite-dimensional \mathcal{RH}_∞ space and provided a proof of its global convergence. Future work should address the scalability of the proposed algorithm to large-scale systems and its robustness against unmodeled dynamics. Furthermore, the preliminary data-driven extension discussed in the appendix suggests a potential path toward model-free implementations, which is a valuable direction for applications where system models are unavailable or inaccurate. In summary, this study analyzes the LQG problem from a policy optimization perspective, contributing to the understanding of the optimization landscape and algorithm design in this area.

Appendix

A Data-Driven Estimation Procedures for Key Operators

Beyond the convergence analysis of Algorithm 1, practical implementation relies on accurately estimating several key system operators when the system parameters are unknown. This subsection briefly describes the estimation methods for the following operators based on input-output data (observation y_t and control input u_t of system (8)):

1. the interconnection operator $\mathbf{M}_{22}^{\mathcal{K}_0}(s)$;
2. the closed-loop sensitivity operator $\mathbf{S}_k(s)$ in Algorithm 1;
3. the residue terms, defined as $\mathbf{e}_{(q+m_1) \times (q+m_2)}(\text{Res}_{\Re(s) \leq 0}(\mathbf{S}_k(s)), m_1, m_2)$.

Detailed numerical analyses and comprehensive performance evaluations of these estimation methods are left for future work.

A.0.1 Estimation of $\mathbf{M}_{22}^{\mathcal{K}_0}$

This subsection aims to estimate the transfer function matrix $\mathbf{M}_{22}^{\mathcal{K}_0}(s)$ via input-output identification. To ensure sufficient excitation of the internal filter dynamics during this process, we augment the filter equation of the overall system (8) by introducing an explicit auxiliary input $u_{\hat{x}t}$:

$$\dot{\hat{x}}_t = A_{\mathcal{K}}\hat{x}_t + B_{\mathcal{K}}y_t + u_{\hat{x}t}.$$

Here, the filter is an artificial component introduced for control synthesis purposes. Its state \hat{x}_t is entirely accessible in simulation (or in numerical experiments), and the input $u_{\hat{x}t}$ can therefore be freely specified to provide targeted excitation for identification, without affecting the underlying physical plant. By introducing the auxiliary input $u_{\hat{x}t}$ into the filter dynamics of (8) and considering a fixed controller $\mathcal{K} = \mathcal{K}_0$, the resulting augmented system has composite input $(u_t, u_{\hat{x}t})$ and output (y_t, \hat{x}_t) . The transfer matrix $\mathbf{M}_{22}^{\mathcal{K}_0}(s)$ is thus defined as the mapping from the input to the output, consistent with the structure in (23).

However, the system (8) is subject to process noise ω_t and measurement noise v_t . It is beneficial to examine the system's input-output behavior in the frequency domain to account for these stochastic effects in both analysis and identification. By taking the Laplace transform of the system equations (8) (with the auxiliary input $u_{\hat{x}t}$ included), we obtain the following input-output relationship:

$$y(s) = \mathbf{M}_{22}^{\mathcal{K}_0}(s) u_{\omega}(s) + w(s), \quad (75)$$

where $y(s)$ is the Laplace transform of output signal (y_t, \hat{x}_t) , $u_{\omega}(s)$ is the Laplace transform of the composite input $(u_t, u_{\hat{x}t})$, $\mathbf{M}_{22}^{\mathcal{K}_0}(s)$ denotes the noise-free transfer operator of interest, and $w(s)$ aggregates the effects of all the noise sources. This frequency-domain representation (75) provides a convenient starting point for empirical identification, as it directly relates the observable output to the known excitation (input) and delineates the influence of stochastic disturbances.

We sequentially apply sinusoidal excitations to each input channel of $(u_t, u_{\hat{x}t})$ for system identification. Specifically, for each $h = 1, \dots, q + m_2$, we use the excitation

$$u_{\omega}(s) = c_{\omega} \frac{\omega}{s^2 + \omega^2} e_{1 \times (q+m_2)}(1, h),$$

where $\frac{\omega}{s^2 + \omega^2}$ is the Laplace transform of $\sin(\omega t)$. Owing to the frequency response properties of linear systems [12], the response of the i -th noise-free output to input $u_{\omega}(s)$ is

$$\mathcal{L}^{-1}(y_{\omega}(s)_i) = c_{\omega} \left| \mathbf{M}_{22}^{\mathcal{K}_0}(j\omega)_{i,h} \right| \sin(\omega t + \arg \mathbf{M}_{22}^{\mathcal{K}_0}(j\omega)_{i,h}), \quad (76)$$

where \mathcal{L}^{-1} denotes the inverse Laplace transform and $y_{\omega}(s)_i$ is the i -th entry of the noise-free output. Provided that c_{ω} is sufficiently large relative to the spectral norm of $w(s)$, the noise term becomes

negligible; after normalizing by c_ω , we obtain

$$\frac{y(s)}{c_\omega} \approx \mathbf{M}_{22}^{\mathcal{K}_0}(s) \frac{\omega}{s^2 + \omega^2} e_{1 \times (q+m_2)}(1, h), \quad (77)$$

enabling accurate empirical estimation of the frequency response for each input-output pair over a frequency grid. Once the empirical frequency response data have been collected, we fit each entry of the transfer function matrix $\mathbf{M}_{22}^{\mathcal{K}_0}(s)$ individually by parameterizing it as a rational function. For each input channel h and output channel i , i.e., for each (i, h) -th entry of $\mathbf{M}_{22}^{\mathcal{K}_0}(s)$, we consider the following parameterization:

$$\mathbf{M}_{22}^{\mathcal{K}_0}(s)_{i,h} \approx \frac{N(s)}{D(s)} = \frac{\sum_{k=0}^{n_{\text{deg},1}} a_k s^k}{\sum_{k=0}^{n_{\text{deg},2}} b_k s^k}, \quad (78)$$

where $N(s)$ and $D(s)$ are polynomials of degree at most $n_{\text{deg},1}$ and $n_{\text{deg},2}$, respectively. Here, the index i corresponds to the i -th output (either y_t or an entry of \hat{x}_t) and h to the h -th input (either u_t or an entry of $u_{\hat{x}t}$) in the composite system. The frequency-domain least-squares problem is formulated as

$$\min_{a_k, b_k} \left\| \frac{\sum_{k=0}^{n_{\text{deg},1}} a_k s^k}{\sum_{k=0}^{n_{\text{deg},2}} b_k s^k} - \mathbf{M}_{22}^{\mathcal{K}_0}(s)_{i,h} \right\|_{\mathcal{H}_2}^2. \quad (79)$$

This problem is nonlinear in the polynomial coefficients due to the rational form. However, in the absence of noise, both the empirical output data and the target transfer function can be matched exactly. Hence, the global optimum achieves zero objective value (i.e., the rational function equals the actual transfer function at all frequencies). In this ideal setting, the optimization problem above reduces to solving

$$\sum_{k=0}^{n_{\text{deg},1}} a_k s^k - \mathbf{M}_{22}^{\mathcal{K}_0}(s)_{i,h} \sum_{k=0}^{n_{\text{deg},2}} b_k s^k = 0, \quad (80)$$

for all the frequency points considered. This motivates the use of the following linearized least-squares surrogate:

$$\min_{a_k, b_k} \left\| \sum_{k=0}^{n_{\text{deg},1}} a_k s^k - \mathbf{M}_{22}^{\mathcal{K}_0}(s)_{i,h} \sum_{k=0}^{n_{\text{deg},2}} b_k s^k \right\|_{\mathcal{H}_2}^2, \quad (81)$$

which is convex in the coefficients and shares the same set of global optimizers as the original problem under noise-free data. Therefore, this convex reformulation preserves the solution in the ideal (noiseless) scenario and remains tractable in practice. This process is repeated for all the $i = 1, \dots, q + m_1$ and $h = 1, \dots, q + m_2$, and the final transfer function matrix is assembled from the individually estimated entries. Additional implementation details can be found in [22, 23, 24, 25].

A.0.2 Estimation of Sensitivity Operators

$\mathbf{S}_k(s)$ represents the Fréchet derivative of the performance index $J_{\mathcal{K}_0}(\mathbf{Q}_k, Q_k)$ with respect to the operator variable \mathbf{Q}_k , as established in Theorem 5.3. Importantly, these operators do not correspond to physical transfer functions. Accordingly, they lack direct physical realizations and cannot be identified through system excitation and output measurement, as is possible for $\mathbf{M}_{22}^{\mathcal{K}_0}$.

We estimate the operator $\mathbf{S}_k(s)$ using an orthogonal basis expansion. The underlying principle is that the operator can be represented as an infinite sum of orthogonal basis functions. In practice, we approximate the operator by truncating this series to a finite number of terms, which transforms the estimation problem into the more tractable task of computing a finite set of generalized coefficients. Each coefficient for this expansion is calculated as the directional derivative of the performance index $J_{\mathcal{K}_0}(\mathbf{Q}_k, Q_k)$ along the direction of its corresponding basis function. This process yields a finite-series approximation of the operator, which serves as a surrogate. Finally, for practical implementation, this surrogate operator is converted into a standard, reduced-order rational transfer function via frequency-domain least-squares fitting, as detailed below.

In our implementation, we specifically select the Laguerre basis functions [1] for this expansion. For each (i, j) entry of $\mathbf{S}_k(s)$, we introduce the following perturbation:

$$\begin{aligned} (\Delta \mathbf{Q}, \Delta Q) &:= \left(c \frac{\sqrt{2a}}{s+a} \left(\frac{s-a}{s+a} \right)^k e_{(q+m_1) \times (q+m_2)}(i, j), 0 \right), \\ i &= 1, 2, \dots, q+m_1, \quad j = 1, 2, \dots, q+m_2, \quad k = 0, 1, 2, \dots \end{aligned} \quad (82)$$

By substituting this into $J_{\mathcal{K}_0}(\mathbf{Q}_k + \Delta \mathbf{Q}, Q_k + \Delta Q)$, the corresponding change in performance is

$$J_{\mathcal{K}_0}(\mathbf{Q}_k + \Delta \mathbf{Q}, Q_k + \Delta Q) = J_{\mathcal{K}_0}(\mathbf{Q}_k, Q_k) + 2 \operatorname{tr} \left(c \int_{-\infty}^{\infty} \Delta \mathbf{Q}(j\omega)^* \mathbf{S}_k(j\omega) d\omega \right) + o(c). \quad (83)$$

In accordance with best approximation theory [11], each (i, j) entry of $\mathbf{S}_k(s)$ can thus be expressed as a linear combination of the orthogonal Laguerre basis functions $\frac{\sqrt{2a}}{s+a} \left(\frac{s-a}{s+a} \right)^k$, where the coefficients $c_k(i, j)$ are given by the \mathcal{H}_2 inner product (projection) of $\mathbf{S}_k(s)_{i,j}$ onto the corresponding basis function. In practice, these coefficients are numerically evaluated as the finite-difference approximation of the directional derivative of $J_{\mathcal{K}_0}$ with respect to c for each basis direction (as reflected in (83)):

$$c_k(i, j) = \lim_{c \rightarrow 0} \frac{J_{\mathcal{K}_0}(\mathbf{Q}_k + \Delta \mathbf{Q}, Q_k + \Delta Q) - J_{\mathcal{K}_0}(\mathbf{Q}_k, Q_k)}{2c}.$$

With these coefficients, each entry $\mathbf{S}_k(s)_{i,j}$ is approximated as a truncated expansion:

$$\hat{\mathbf{S}}_k(s)_{i,j} = \sum_{k=0}^N c_k(i, j) \frac{\sqrt{2a}}{s+a} \left(\frac{s-a}{s+a} \right)^k,$$

where N is the chosen truncation order. To address the potential complexity arising from high-order models, each entry $\mathbf{S}_k(s)_{i,j}$ is further approximated by a reduced-order rational transfer function of the form

$$\frac{\sum_{k=0}^{n_{\text{deg},1}} a_k s^k}{\sum_{k=0}^{n_{\text{deg},2}} b_k s^k}$$

via a frequency-domain least-squares fitting. Here, $n_{\text{deg},1}$ and $n_{\text{deg},2}$ are user-specified maximal orders. Specifically, for each input-output pair (i, j) , we solve

$$\min_{a_k, b_k} \left\| \frac{\sum_{k=0}^{n_{\text{deg},1}} a_k s^k}{\sum_{k=0}^{n_{\text{deg},2}} b_k s^k} - \hat{\mathbf{S}}_k(s)_{i,j} \right\|_{\mathcal{H}_2}^2. \quad (84)$$

This can also be reformulated as the following convex optimization problem, provided N is sufficiently large to make the truncation error negligible:

$$\min_{a_k, b_k} \left\| \sum_{k=0}^{n_{\text{deg},1}} a_k s^k - \hat{\mathbf{S}}_k(s)_{i,j} \sum_{k=0}^{n_{\text{deg},2}} b_k s^k \right\|_{\mathcal{H}_2}^2. \quad (85)$$

This optimization is carried out for all $i = 1, 2, \dots, q+m_1$ and $j = 1, 2, \dots, q+m_2$, resulting in the reduced-order rational approximations for all entries of $\mathbf{S}_k(s)$. Each entry thus takes the form $\sum_{k=0}^{n_{\text{deg},1}} a_k s^k / \sum_{k=0}^{n_{\text{deg},2}} b_k s^k$, and the matrix-valued transfer function $\mathbf{S}_k(s)$ are assembled accordingly.

A.0.3 Estimation of Residue Terms

To estimate the residue term $\mathbf{e}_{(q+m_1) \times (q+m_2)}(\operatorname{Res}_{\Re(s) \leq 0}(\mathbf{S}_k(s)), m_1, m_2)$, we employ zeroth-order (gradient-free) methods [10, 21].

According to Theorem 5.3, we have

$$\nabla_{Q_k} J_{\mathcal{K}_0}(\mathbf{Q}_k, Q_k) = 2 \mathbf{e}_{(q+m_1) \times (q+m_2)}(\operatorname{Res}_{\Re(s) \leq 0}(\mathbf{S}_k(s)), m_1, m_2). \quad (86)$$

Using zeroth-order methods (see, e.g., Sec. D.3 in [9]), the gradient can be estimated as

$$\nabla_{Q_k} J_{\mathcal{K}_0}(\mathbf{Q}_k, Q_k) = \frac{d}{2r^2} \mathbb{E}_{U \sim \operatorname{Unif}(\mathbb{S}_r)} [(J_{\mathcal{K}_0}(\mathbf{Q}_k, Q_k + U) - J_{\mathcal{K}_0}(\mathbf{Q}_k, Q_k - U))U], \quad (87)$$

where \mathbb{S}_r denotes the surface of the sphere with radius r (under the spectral norm) in $\mathbb{R}^{(q+m_1) \times (q+m_2) | m_1 \times m_2}$, $\text{Unif}(\mathbb{S}_r)$ denotes the uniform distribution over \mathbb{S}_r , and d is the dimension of Q_k . Given independent and identical distributed samples $U_1, \dots, U_m \sim \text{Unif}(\mathbb{S}_r)$, we approximate the expectation in (87) empirically by

$$\hat{\nabla}_{Q_k} J_{\mathcal{K}_0}(\mathbf{Q}_k, Q_k) = \frac{1}{m} \sum_{i=1}^m \frac{d}{2r^2} (J_{\mathcal{K}_0}(\mathbf{Q}_k, Q_k + U_i) - J_{\mathcal{K}_0}(\mathbf{Q}_k, Q_k - U_i)) U_i. \quad (88)$$

This estimation methodology has been widely adopted in the optimal control literature [8, 9, 13, 30].

B Second-Order Optimality Condition

By combining Theorem 3.4 in this paper with Theorem 2 in [41], we characterize the optimality condition in terms of the second-order derivatives of the objective function in (8). This result is formalized in the following corollary. To simplify the presentation, for any controller $\mathcal{K} \in \mathbb{K}_q$ and any positive integer p , we define the augmented controller

$$\tilde{\mathcal{K}}(\lambda) := \left[\begin{array}{c|cc} 0 & C_{\mathcal{K}} & 0 \\ \hline B_{\mathcal{K}} & A_{\mathcal{K}} & 0 \\ 0 & 0 & \lambda I_p \end{array} \right], \lambda \in \mathbb{R}$$

and the corresponding set

$$\mathcal{M}_p := \left\{ \Delta = \left[\begin{array}{c|cc} 0 & 0 & \Delta_C \\ \hline 0 & 0 & \Delta_{A1} \\ \Delta_B & \Delta_{A2} & \Delta_{A3} \end{array} \right], \Delta_B \in \mathbb{R}^{p \times m_2}, \Delta_{A1} \in \mathbb{R}^{q \times p}, \Delta_{A2} \in \mathbb{R}^{p \times q}, \Delta_{A3} \in \mathbb{R}^{p \times p}, \Delta_C \in \mathbb{R}^{m_1 \times p} \right\}.$$

Corollary B.1. *Let $\mathcal{K} \in \mathbb{K}_q$ and p be a positive integer. Then, \mathcal{K} is a global optimal solution to the problem (8) if and only if the second-order directional derivative of $J(\tilde{\mathcal{K}}(\lambda))$ with respect to Δ is identically zero, i.e.,*

$$D_{\Delta}^2 J(\tilde{\mathcal{K}}(\lambda)) = 0, \quad \forall \lambda \in \mathbb{R}, \Delta \in \mathcal{M}_p. \quad (89)$$

Moreover, if \mathcal{K} is not a global optimal solution to problem (8), there exist $\Delta \in \mathcal{M}_p$ and $\lambda \in \mathbb{R}$ such that $D_{\Delta}^2 J(\tilde{\mathcal{K}}(\lambda)) < 0$.

Proof. Based on Lemma 3 of [41], $D_{\Delta}^2 J(\tilde{\mathcal{K}}(\lambda))$ in the direction of

$$\Delta = \left[\begin{array}{c|cc} 0 & 0 & \Delta_C \\ \hline 0 & 0 & \Delta_{A1} \\ \Delta_B & \Delta_{A2} & \Delta_{A3} \end{array} \right] \in \mathcal{M}_p$$

can be expressed as

$$D_{\Delta}^2 J(\tilde{\mathcal{K}}(\lambda)) = 2 \text{tr} \left(2 \begin{bmatrix} \Sigma_{\mathcal{K}} & 0 \\ 0 & 0 \end{bmatrix} P'_{\mathcal{K}, \Delta} \begin{bmatrix} 0 & 0 & B\Delta_C \\ 0 & 0 & \Delta_{A1} \\ \Delta_B C & \Delta_{A2} & \Delta_{A3} \end{bmatrix} + 2P'_{\mathcal{K}, \Delta} \begin{bmatrix} 0 & 0 & 0 \\ 0 & 0 & B_{\mathcal{K}} \mathcal{V} \Delta_B^{\top} \\ 0 & 0 & 0 \end{bmatrix} \right).$$

Here, $\mathcal{P}_{\mathcal{K}}$ and $\Sigma_{\mathcal{K}}$ are the solutions to the Lyapunov equations (12), and $P'_{\mathcal{K}, \Delta} \in \mathbb{R}^{(n+q+p) \times (n+q+p)}$ is the solution to the following Lyapunov equation

$$\begin{bmatrix} A & BC_{\mathcal{K}} & 0 \\ BC_{\mathcal{K}} & A_{\mathcal{K}} & 0 \\ 0 & 0 & \lambda I_p \end{bmatrix}^{\top} P'_{\mathcal{K}, \Delta} + P'_{\mathcal{K}, \Delta} \begin{bmatrix} A & BC_{\mathcal{K}} & 0 \\ BC_{\mathcal{K}} & A_{\mathcal{K}} & 0 \\ 0 & 0 & \lambda I_p \end{bmatrix} + M_1(\mathcal{P}_{\mathcal{K}}, \Delta) = 0 \quad (90)$$

with

$$M_1(\mathcal{P}_{\mathcal{K}}, \Delta) := \begin{bmatrix} 0 & 0 & B\Delta_C \\ 0 & 0 & \Delta_{A1} \\ \Delta_B C & \Delta_{A2} & \Delta_{A3} \end{bmatrix}^{\top} \begin{bmatrix} \mathcal{P}_{\mathcal{K}} & 0 \\ 0 & 0 \end{bmatrix} + \begin{bmatrix} \mathcal{P}_{\mathcal{K}} & 0 \\ 0 & 0 \end{bmatrix} \begin{bmatrix} 0 & 0 & B\Delta_C \\ 0 & 0 & \Delta_{A1} \\ \Delta_B C & \Delta_{A2} & \Delta_{A3} \end{bmatrix} \\ + \begin{bmatrix} 0 & 0 & 0 \\ 0 & 0 & C_{\mathcal{K}}^{\top} R \Delta_C \\ 0 & \Delta_C^{\top} R C_{\mathcal{K}} & 0 \end{bmatrix}.$$

We now decompose the direction Δ into four parts:

$$\Delta^{(1)} = \left[\begin{array}{c|cc} 0 & 0 & \Delta_C \\ \hline 0 & 0 & 0 \\ 0 & 0 & 0 \end{array} \right], \Delta^{(2)} = \left[\begin{array}{c|cc} 0 & 0 & 0 \\ \hline 0 & 0 & 0 \\ \Delta_B & 0 & 0 \end{array} \right], \Delta^{(3)} = \left[\begin{array}{c|cc} 0 & 0 & 0 \\ \hline 0 & 0 & 0 \\ 0 & 0 & \Delta_{A3} \end{array} \right], \Delta^{(4)} = \left[\begin{array}{c|cc} 0 & 0 & 0 \\ \hline 0 & 0 & \Delta_{A1} \\ 0 & \Delta_{A2} & 0 \end{array} \right].$$

With these definitions, $D_{\Delta}^2 J(\tilde{\mathcal{K}}(\lambda))$ expands as

$$\begin{aligned} D_{\Delta}^2 J(\tilde{\mathcal{K}}(\lambda)) &= D_{\Delta^{(1)}+\Delta^{(2)}+\Delta^{(3)}}^2 J(\tilde{\mathcal{K}}(\lambda)) + 2D_{\Delta^{(3)}} D_{\Delta^{(4)}} J(\tilde{\mathcal{K}}(\lambda)) \\ &\quad + 2D_{\Delta^{(1)}+\Delta^{(2)}} D_{\Delta^{(4)}} J(\tilde{\mathcal{K}}(\lambda)) + D_{\Delta^{(4)}}^2 J(\tilde{\mathcal{K}}(\lambda)). \end{aligned}$$

Define the transfer function matrices

$$\begin{aligned} \mathbf{H}_{11} &:= (B^{\top} P_1^{\mathcal{K}} + R\bar{C}_{\mathcal{K}})(sI - \mathcal{A})^{-1}((C\Sigma_1^{\mathcal{K}})^{\top} + \bar{B}_{\mathcal{K}}\mathcal{V}), \quad \mathbf{H}_{12} := (B^{\top} P_1^{\mathcal{K}} + R\bar{C}_{\mathcal{K}})(sI - \mathcal{A})^{-1}\Sigma_2^{\mathcal{K}\top}, \\ \mathbf{H}_{21} &:= P_2^{\mathcal{K}}(sI - \mathcal{A})^{-1}((C\Sigma_1^{\mathcal{K}})^{\top} + \bar{B}_{\mathcal{K}}\mathcal{V}), \quad \mathbf{H}_{22} := P_2^{\mathcal{K}}(sI - \mathcal{A})^{-1}\Sigma_2^{\mathcal{K}\top}. \end{aligned}$$

Then, the optimality condition (27) is equivalent to

$$(\mathcal{C}_1 - \mathcal{B}_1 \mathcal{P}_{\mathcal{K}})(sI - \mathcal{A})^{-1}(\mathcal{B}_0 - \Sigma_{\mathcal{K}} \mathcal{C}_0) = \begin{bmatrix} \mathbf{H}_{11} & \mathbf{H}_{12} \\ \mathbf{H}_{21} & \mathbf{H}_{22} \end{bmatrix} \equiv 0, \quad \forall s \in \mathbb{C}.$$

To complete the proof, it remains to show the equivalence between the condition

$$D_{\Delta}^2 J(\tilde{\mathcal{K}}(\lambda)) \equiv 0, \quad \forall \lambda \in \mathbb{R}, \Delta \in \mathcal{M}_p$$

and the condition (27), i.e.,

$$\mathbf{H}_{11} \equiv \mathbf{H}_{12} \equiv \mathbf{H}_{21} \equiv \mathbf{H}_{22} \equiv 0, \quad \forall s \in \mathbb{C}.$$

Theorem 2 of [41] implies that the first term $D_{\Delta^{(1)}+\Delta^{(2)}+\Delta^{(3)}}^2 J(\tilde{\mathcal{K}}(\lambda)) \equiv 0, \forall \lambda \in \mathbb{R}, \Delta \in \mathcal{M}_p$ if and only if $\mathbf{H}_{11} \equiv 0, \forall s \in \mathbb{C}$. We therefore only analyze the subsequent terms $D_{\Delta^{(4)}}^2 J(\tilde{\mathcal{K}}(\lambda)), D_{\Delta^{(1)}+\Delta^{(2)}} D_{\Delta^{(4)}} J(\tilde{\mathcal{K}}(\lambda))$ and $D_{\Delta^{(3)}} D_{\Delta^{(4)}} J(\tilde{\mathcal{K}}(\lambda))$. First, for $D_{\Delta^{(4)}}^2 J(\tilde{\mathcal{K}}(\lambda))$, it holds that

$$M_1(\mathcal{P}_{\mathcal{K}}, \Delta^{(4)}) = \begin{bmatrix} 0 & 0 & P_{12}^{\mathcal{K}} \Delta_{A1} \\ 0 & 0 & P_{22}^{\mathcal{K}} \Delta_{A1} \\ \Delta_{A1}^{\top} (P_{12}^{\mathcal{K}})^{\top} & \Delta_{A1}^{\top} P_{22}^{\mathcal{K}} & 0 \end{bmatrix}. \quad (91)$$

Taking (91) into $D_{\Delta^{(4)}}^2 J(\tilde{\mathcal{K}}(\lambda))$ and using the Lyapunov equation (90), we have

$$\begin{aligned} &D_{\Delta^{(4)}}^2 J(\tilde{\mathcal{K}}(\lambda)) \\ &= 4 \int_0^{\infty} \text{tr} \left(\begin{bmatrix} 0 & \exp(\mathcal{A}^{\top} t) (P_2^{\mathcal{K}})^{\top} \Delta_{A1} \exp(\lambda t) \\ \Delta_{A1}^{\top} \exp(\lambda t) P_2^{\mathcal{K}} \exp(\mathcal{A} t) & 0 \end{bmatrix} \Delta^{(4)} \begin{bmatrix} \Sigma_{\mathcal{K}} & 0 \\ 0 & 0 \end{bmatrix} \right) dt \\ &= 4 \int_0^{\infty} \text{tr} \left(\begin{bmatrix} 0 & 0 \\ 0 & \Delta_{A1}^{\top} P_2^{\mathcal{K}} \exp((\lambda I + \mathcal{A}) t) (\Sigma_2^{\mathcal{K}})^{\top} \Delta_{A2}^{\top} \end{bmatrix} \right) dt. \end{aligned} \quad (92)$$

According to (92), it follows that $D_{\Delta^{(4)}}^2 J(\tilde{\mathcal{K}}(\lambda)) \equiv 0, \forall \lambda \in \mathbb{R}, \Delta \in \mathcal{M}_p$ if and only if $\mathbf{H}_{22} \equiv 0, \forall s \in \mathbb{C}$.

By similar arguments, for $D_{\Delta^{(1)}+\Delta^{(2)}} D_{\Delta^{(4)}} J(\tilde{\mathcal{K}}(\lambda))$, we have

$$\begin{aligned} D_{\Delta^{(1)}+\Delta^{(2)}} D_{\Delta^{(4)}} J(\tilde{\mathcal{K}}(\lambda)) &= 4 \int_0^{\infty} \text{tr} \left(\begin{bmatrix} 0 & 0 \\ 0 & \Delta_C^{\top} (B^{\top} P_1^{\mathcal{K}} + R\bar{C}_{\mathcal{K}}) \exp((\lambda I + \mathcal{A}) t) (\Sigma_2^{\mathcal{K}})^{\top} \Delta_{A2}^{\top} \end{bmatrix} \right) dt \\ &\quad + 4 \int_0^{\infty} \text{tr} \left(\begin{bmatrix} 0 & 0 \\ 0 & \Delta_{A1}^{\top} P_2^{\mathcal{K}} \exp((\lambda I + \mathcal{A}) t) (C\Sigma_1^{\mathcal{K}} + \mathcal{V}\bar{B}_{\mathcal{K}}^{\top})^{\top} \Delta_B^{\top} \end{bmatrix} \right) dt. \end{aligned} \quad (93)$$

Equation (93) implies that the condition $D_{\Delta^{(1)}+\Delta^{(2)}} D_{\Delta^{(4)}} J(\tilde{\mathcal{K}}(\lambda)) \equiv 0, \forall \lambda \in \mathbb{R}, \Delta \in \mathcal{M}_p$ holds if and only if $\mathbf{H}_{12} \equiv \mathbf{H}_{21} \equiv 0, \forall s \in \mathbb{C}$. Furthermore, for $D_{\Delta^{(3)}} D_{\Delta^{(4)}} J(\tilde{\mathcal{K}}(\lambda))$, it holds that

$$D_{\Delta^{(3)}} D_{\Delta^{(4)}} J(\tilde{\mathcal{K}}(\lambda)) = 4 \text{tr} \left(\begin{bmatrix} \Sigma_{\mathcal{K}} & 0 \\ 0 & 0 \end{bmatrix} P'_{\mathcal{K}, \Delta^{(4)}} \begin{bmatrix} 0 & 0 & 0 \\ 0 & 0 & 0 \\ 0 & 0 & \Delta_{A3} \end{bmatrix} \right)$$

$$+ 4 \operatorname{tr} \left(\begin{bmatrix} \Sigma_{\mathcal{K}} & 0 \\ 0 & 0 \end{bmatrix} P'_{\mathcal{K}, \Delta^{(3)}} \begin{bmatrix} 0 & 0 & 0 \\ 0 & 0 & \Delta_{A1} \\ 0 & \Delta_{A2} & 0 \end{bmatrix} \right) \equiv 0, \forall \lambda \in \mathbb{R}, \Delta \in \mathcal{M}_p.$$

In conclusion, $D_{\Delta}^2 J(\tilde{\mathcal{K}}(\lambda)) \equiv 0$ for any $\lambda \in \mathbb{R}$, $\Delta \in \mathcal{M}_p$ if and only if the condition (27) holds. Meanwhile, based on the specific forms of the derivatives, when (89) does not hold, it is evident that there exist $\Delta \in \mathcal{M}_p$ and $\lambda \in \mathbb{R}$ such that $D_{\Delta}^2 J(\tilde{\mathcal{K}}(\lambda)) < 0$. This completes the proof. \square

References

- [1] Osvaldo Agamennoni, Eduardo Paolini, and Alfredo Desages. On robust stability analysis of a control system using laguerre series. *Automatica*, 28(4):815–818, 1992.
- [2] Pierre. Apkarian and Dominikus. Noll. Nonsmooth \mathcal{H}_{∞} synthesis. *IEEE Transactions on Automatic Control*, 51(1):71–86, 2006.
- [3] Dimitri Bertsekas. *Dynamic Programming and Optimal Control*, volume 1. 01 1995.
- [4] Jean-Pierre Corriou. *Optimal Control*, pages 493–554. Springer London, London, 2004.
- [5] John C. Doyle. Guaranteed margins for LQG regulators. *IEEE Transactions on Automatic Control*, 23(4):756–757, 1978.
- [6] Jingliang Duan, Wenhan Cao, Yang Zheng, and Lin Zhao. On the optimization landscape of dynamic output feedback linear quadratic control. *IEEE Transactions on Automatic Control*, 69(2):920–935, 2024.
- [7] Ilyas Fatkhullin and Boris Polyak. Optimizing static linear feedback: Gradient method. *SIAM J. Control. Optim.*, 59:3887–3911, 2020.
- [8] Maryam Fazel, Rong Ge, Sham Kakade, and Mehran Mesbahi. Global convergence of policy gradient methods for the linear quadratic regulator. In *Proceedings of the 35th International Conference on Machine Learning*, volume 80 of *Proceedings of Machine Learning Research*, pages 1467–1476. PMLR, 10–15 2018.
- [9] Maryam Fazel, Rong Ge, Sham M. Kakade, and Mehran Mesbahi. Global convergence of policy gradient methods for the linear quadratic regulator. In *International Conference on Machine Learning*, 2018.
- [10] Abraham D. Flaxman, Adam Tauman Kalai, and H. Brendan. McMahan. Online convex optimization in the bandit setting: gradient descent without a gradient.
- [11] Walter Gautschi. *Approximation and Interpolation*, pages 55–158. Birkhäuser Boston, Boston, 2012.
- [12] Graham C. Goodwin, Stefan F. Graebe, and Mario E. Salgado. *Control System Design*. Prentice Hall PTR, USA, 1st edition, 2000.
- [13] Ben Hambly, Renyuan Xu, and Huining Yang. Policy gradient methods for the noisy linear quadratic regulator over a finite horizon. *SIAM Journal on Control and Optimization*, 59(5):3359–3391, 2021.
- [14] Mingyi Hong, Zhi-Quan Luo, and Meisam Razaviyayn. Convergence analysis of alternating direction method of multipliers for a family of nonconvex problems. *SIAM Journal on Optimization*, 26(1):337–364, 2016.
- [15] Bin. Hu, Kaiqing. Zhang, Na. Li, Mehran Mesbahi, Maryam Fazel, and Tamer Bacsar. Towards a theoretical foundation of policy optimization for learning control policies. *ArXiv*, abs/2210.04810, 2022.
- [16] Joao Paulo Jansch-Porto, Bin Hu, and Geir E. Dullerud. Policy optimization for markovian jump linear quadratic control: Gradient method and global convergence. *IEEE Transactions on Automatic Control*, 68(4):2475–2482, 2023.

- [17] Imane Mahtout, Francisco Navas, Vicente Milanés, and Fawzi Nashashibi. Advances in youla-kucera parametrization: A review. *Annual Reviews in Control*, 49:81–94, 2020.
- [18] Volodymyr Mnih et al. Human-level control through deep reinforcement learning. *Nature*, 518(7540):529–533, 2015.
- [19] Hesameddin Mohammadi, Armin Zare, Mahdi Soltanolkotabi, and Mihailo R. Jovanović. Convergence and sample complexity of gradient methods for the model-free linear–quadratic regulator problem. *IEEE Transactions on Automatic Control*, 67:2435–2450, 2019.
- [20] Yurii Nesterov. *Smooth Convex Optimization*, pages 59–137. Springer International Publishing, Cham, 2018.
- [21] Yurii Nesterov and Vladimir Spokoiny. Random gradient-free minimization of convex functions. *Foundations of Computational Mathematics*, 17(2):527–566, 2017.
- [22] Rik Pintelon and Johan Schoukens. *Design of Excitation Signals*, pages 151–175. 2012.
- [23] Rik Pintelon and Johan Schoukens. *Frequency Response Function Measurements in the Presence of Nonlinear Distortions*, pages 73–118. 2012.
- [24] Rik Pintelon and Johan Schoukens. *Measurement of Frequency Response Functions - The Local Polynomial Approach*, pages 225–278. 2012.
- [25] Rik Pintelon, Johan Schoukens, and Gerd Vandersteen. Frequency domain system identification using arbitrary signals. *IEEE Transactions on Automatic Control*, 42(12):1717–1720, 1997.
- [26] Aravind Rajeswaran, Vikash Kumar, Abhishek Gupta, Giulia Vezzani, John Schulman, Emanuel Todorov, and Sergey Levine. Learning complex dexterous manipulation with deep reinforcement learning and demonstrations, 2018.
- [27] Benjamin Recht. A tour of reinforcement learning: The view from continuous control. *Annual Review of Control, Robotics, and Autonomous Systems*, 2, 05 2019.
- [28] Carsten Scherer, Pascal Gahinet, and Mahmoud Chilali. Multiobjective output-feedback control via lmi optimization. *IEEE Transactions on Automatic Control*, 42(7):896–911, 1997.
- [29] David Silver, Aja Huang, Chris Maddison, et al. Mastering the game of Go with deep neural networks and tree search. *Nature*, 529(7587):484–489, 2016.
- [30] Yujie Tang, Yang Zheng, and Na Li. Analysis of the optimization landscape of linear quadratic gaussian (LQG) control. In *Proceedings of the 3rd Conference on Learning for Dynamics and Control*, volume 144 of *Proceedings of Machine Learning Research*, pages 599–610. PMLR, 07 – 08 June 2021.
- [31] Yujie Tang, Yang Zheng, and Na Li. Analysis of the optimization landscape of linear quadratic gaussian (lqg) control. *Mathematical Programming*, 202(1):399–444, Nov 2023.
- [32] Jack Umenberger, Max Simchowitz, Juan Perdomo, Kaiqing Zhang, and Russ Tedrake. Globally convergent policy search over dynamic filters for output estimation. *ArXiv*, abs/2202.11659, 2022.
- [33] Dante Youla and Joseph Bongiorno. A feedback theory of two-degree-of-freedom optimal wiener-hopf design. *IEEE Transactions on Automatic Control*, 30(7):652–665, 1985.
- [34] Dante Youla, Hamid Jabr, and Joseph Bongiorno. Modern wiener-hopf design of optimal controllers—part II: The multivariable case. *IEEE Transactions on Automatic Control*, 21(3):319–338, 1976.
- [35] Kaiqing Zhang, Bin Hu, and Tamer Başar. Policy optimization for \mathcal{H}_2 linear control with \mathcal{H}_∞ robustness guarantee: Implicit regularization and global convergence, 2021.
- [36] Yufeng Zhang, Zhuoran Yang, and Zhaoran Wang. Provably efficient actor-critic for risk-sensitive and robust adversarial rl: A linear-quadratic case. In *International Conference on Artificial Intelligence and Statistics*, 2021.

- [37] Feiran Zhao, Keyou You, and Tamer Başar. Global convergence of policy gradient primal–dual methods for risk-constrained LQRs. *IEEE Transactions on Automatic Control*, 68(5):2934–2949, 2023.
- [38] Yang Zheng, Luca Furieri, Antonis Papachristodoulou, Na Li, and Maryam Kamgarpour. On the equivalence of youla, system-level, and input–output parameterizations. *IEEE Transactions on Automatic Control*, 66(1):413–420, 2021.
- [39] Yang Zheng, Chih-Fan Pai, and Yujie Tang. Benign nonconvex landscapes in optimal and robust control, part I: Global optimality, 2023. arXiv:2312.15332 [math.OC]. <https://arxiv.org/abs/2312.15332>.
- [40] Yang Zheng, Chih-Fan Pai, and Yujie Tang. Benign nonconvex landscapes in optimal and robust control, part II: Extended convex lifting, 2024. arXiv:2406.04001 [math.OC]. <https://arxiv.org/abs/2406.04001>.
- [41] Yang Zheng, Yue Sun, Maryam Fazel, and Na Li. Escaping high-order saddles in policy optimization for linear quadratic gaussian (LQG) control. In *2022 IEEE 61st Conference on Decision and Control (CDC)*, pages 5329–5334, 2022.
- [42] Kemin Zhou, John C. Doyle, and Keith Glover. Robust and optimal control. *Springer London*, 1995.